AFRL-SR-AR-TR-06-0468

# REPORT DOCUMENTATION PAGE



| 1. REPORT DATE *(DD-MM-YYYY)* | 2. REPORT TYPE | 3. DATES COVERED *(From - To)* |
|---|---|---|
| 09-14-2006 | Final Technical | 16-12-2003 - 14-6-2006 |

**4. TITLE AND SUBTITLE**
(U) A New Class of Hybrid Schemes Based on Large Eddy Simulation and Low-Dimensional Stochastic Models

**5a. CONTRACT NUMBER**

**5b. GRANT NUMBER**
F49620-03-1-0023

**5c. PROGRAM ELEMENT NUMBER**
61102F

**6. AUTHOR(S)**
Tarek Echekki

**5d. PROJECT NUMBER**
2308

**5e. TASK NUMBER** BX

**5f. WORK UNIT NUMBER**

**7. PERFORMING ORGANIZATION NAME(S) AND ADDRESS(ES)**
North Carolina State
University, 2701 Sullivan
Drive, Suite 240
Raleigh, NC 27695-7514

**8. PERFORMING ORGANIZATION REPORT NUMBER**

**9. SPONSORING / MONITORING AGENCY NAME(S) AND ADDRESS(ES)**
AFOSR/NA
875 Randolph St
Suite 325, Room 3112
Arlington, VA 22203
Dr. Julian Tishkoff

**10. SPONSOR/MONITOR'S ACRONYM(S)**

**11. SPONSOR/MONITOR'S REPORT NUMBER(S)**

**12. DISTRIBUTION / AVAILABILITY STATEMENT**
Approved for public release; distribution is unlimited

**13. SUPPLEMENTARY NOTES**

**14. ABSTRACT**
A hybrid approach for large-eddy simulations (LES) of turbulent combustion with the One-Dimensional Turbulence (ODT) model is developed. The need for a structure-based approach can address some of the key challenges arising in the prediction of non-linear physics on the subgrid scale. The implementation involves hybrid solutions of 3D LES with 1D solutions based on the ODT, with ODT elements embedded within the LES computational domain. The solutions require the coupling of LES and ODT as well as the coupling of the different ODT 'processes'. The proposed methodology represents a fundamentally new framework to address subgrid scale physics where statistical information cannot be represented in LES-resolved physics or cannot be assumed *a priori*. Numerical implementation issues are addressed, including a novel implementation of filtered advection for scalars and momentum. Validation studies based on the non-homogeneous autoignition show that the proposed framework and specific implementations yield excellent predictions of the physics.

**15. SUBJECT TERMS**
Turbulent combustion, large-eddy simulations; reacting flows, the One-Dimensional Turbulence (ODT) model, subgrid scale modeling

| 16. SECURITY CLASSIFICATION OF: | | | 17. LIMITATION OF ABSTRACT | 18. NUMBER OF PAGES | 19a. NAME OF RESPONSIBLE PERSON |
|---|---|---|---|---|---|
| a. REPORT | b. ABSTRACT | c. THIS PAGE | | | Dr. Julian M. Tishkoff |
| Unclassified | Unclassified | Unclassified | UL | 43 | 19b. TELEPHONE NUMBER *(include area code)* (703) 696 8478 |

# A New Class of Hybrid Schemes Based on Large Eddy Simulation and Low-Dimensional Stochastic Models

Principal Investigator:

Tarek Echekki
Department of Mechanical and Aerospace Engineering
North Carolina State University
Raleigh, NC 27695-7910

Grant Number: **F49620-03-1-0023**



Final Performance Report
Reporting Period: 16/12/2003-14/6/2006

# A New Class of Hybrid Schemes Based on Large Eddy Simulation and Low-Dimensional Stochastic Models

Principal Investigator: Tarek Echekki
Department of Mechanical and Aerospace Engineering
North Carolina State University
Raleigh, NC 27695-7910

Final Technical Report

## Abstract

A hybrid approach for large-eddy simulations (LES) of turbulent combustion with the One-Dimensional Turbulence (ODT) model is developed. The need for a structure-based approach can address some of the key challenges arising in the prediction of non-linear physics on the subgrid scale. The implementation involves hybrid solutions of 3D LES with 1D solutions based on the ODT, with ODT elements embedded within the LES computational domain. The solutions require the coupling of LES and ODT as well as the coupling of the different ODT "processes." The proposed methodology represents a fundamentally new framework to address subgrid scale physics where statistical information cannot be represented in LES-resolved physics or cannot be assumed *a priori*. Numerical implementation issues are addressed, including a novel implementation of filtered advection for scalars and momentum. Validation studies based on the non-homogeneous autoignition show that the proposed framework and specific implementations yield excellent predictions of the physics.

## I. Introduction

Momentum transport, scalar mixing, and combustion in turbulent flows are governed by multiscale processes. The multiscale nature of these flows has given rise to an increasingly popular simulation approach, large-eddy simulations (LES). The solution approach in LES is based on coarse-grained simulations, where physical phenomena are resolved down to a prescribed cut-off length scale, and the contribution of unresolved subgrid scales is modeled. Inherent in the original LES formulation is the assumption that the physics under consideration, which is associated with momentum and scalar transport, is governed by large-scale motion, while small scales have universal characters. Moreover, the contributions of small scales to the resolved scalar and vector fields are assumed to be primarily dissipative.

In recent years, there has been increased interest in applying LES to turbulent mixing and combustion flows; however, important statistics related to these flows may be governed by subgrid scale processes due to the strong coupling between transport and chemistry. Traditional approaches to evaluate the resolved turbulent transport for momentum and scalars are based on gradient diffusion approximations for the subgrid stresses and the Reynolds fluxes (e.g. the Smagorinsky model, Smagorinsky, 1963 and the dynamic model, Germano *et al.,* 1991); and similar trends have been adopted for reacting flows

(e.g. Cook & Riley, 1994; Pierce & Moin, 1998). Serious limitations of gradient diffusion models have been identified for turbulent mixing and combustion problems, including the presence of different scaling rules for the scalar spectra (Warhaft, 2001) and scalar counter-gradient diffusion (Bray *et al.*, 1985; Poinsot *et al.*, 1996; Veynante *et al.*, 1997; Caldeira-Pires & Heitor, 2001) in flames. Moreover, the evaluation of non-linear source terms, due to reaction, presents additional challenges. Statistical approaches have been developed to address closure for the source term; however, such approaches are inherently limited by the transient nature of the combustion problem, the importance of statistical outliers in determining combustion behavior, and transitions in combustion modes.

The principal challenges for the LES of turbulent mixing and combustion are the representation of transport, chemistry and the coupling of these two processes over a wide range of time and length scales. Two examples of such challenges are illustrated below:

(1) The structure and dynamics of turbulent sooting flames and fires are dependent on radiation from these flames. This radiation is, in turn, dependent on where soot resides within these flames. Strong, non-uniform temperature variations within the flames over distances of the order of tens to hundreds of microns are modulated by curvature and strain effects due to turbulence. A statistical representation may not capture the flame structure-dependent phenomena easily.

(2) During the autoignition of fuel-oxidizer mixtures, autoignition occurs in discrete sites or kernels of which only a fraction evolves into ignition fronts. High and localized dissipation rates result in failed autoignition at the remaining sites. Statistics that represent mean dissipation rates on scalar fluctuations may not be able to capture the high rates of dissipation contribution.

The direct simulation of subgrid scale processes may provide the only robust approaches for representing them accurately; however, such approaches may appear to conflict with the basic underlying LES paradigm: the solution for only a select range of length and time scales. The answer lies in the fact that we are primarily and ultimately interested in statistics and not necessarily the detail of the flow and scalar fields, such as the ones generated during a direct numerical simulation (DNS); therefore, a reasonable representation of these statistics, albeit at a reduced dimension or parameter space, may be sufficient to address the closure problem.

In combustion flows, many structure-based models have been proposed to address primarily the closure for the non-linear reaction source terms in the scalar equations. The classical flamelet approach and later refinements (Peters, 2000) represent examples of representation of the complex turbulent flame structure through surrogate models of simplified laminar flames. Of relevance to our present work are two relatively more recent models, the filtered-density function (FDF) approach (Pope, 1993; Gao & O'Brien, 1993; Collucci *et al.*, 1998; Jaberi *et al.*, 1996, 1999; Giquel & Givi, 2000; Zhou & Pereira, 2000; El Sheikhi *et al.*, 2003) and the LES-LEM approach by Menon and co-workers and McMurtry & co-workers (McMurtry *et al.*, 1992; Menon *et al.*, 1993; Calhoon & Menon, 1996, 1997; Smith & Menon, 1997, 1998; Sankaran & Menon, 2000; Chakravarthy & Menon, 2000, 2001).

The FDF approach evolves from the transported probability density function (PDF) approach that has been successfully implemented in Reynolds-Averaged Navier-Stokes (RANS) simulations (Pope, 1986). As in PDF methods, FDF requires the transport of representative particles. Chemistry is implemented in integrated in closed form; while, mixing is implemented using a mixing model. Transport of these particles is implemented using the LES resolved velocity field, while both velocity fluctuations and molecular diffusive are represented using stochastic processes.

The Linear-Eddy Model (LEM), which was developed originally by Kerstein (1989, 1990, 1991, and 1992) is a one-dimensional mixing model that incorporates molecular processes (with structure) in a deterministic way through solutions of unsteady reaction-diffusion equations and represents turbulent transport stochastically through stirring events. A stirring event on a selected eddy is implemented through a 'triplet-map'. Triplet maps are designed to emulate the compressive-strain and rotational-folding effects of turbulent eddies. The rates and locations of these stirring events are determined by an assumed shape of the kinetic energy spectrum.

The two modeling approaches, FDF and LES-LEM, offer important advantages over traditional approaches, as they potentially can address more general combustion problems involving different burning modes (e.g. premixed vs. nonpremixed) and transitions in the burning modes, burning regime and dominant combustion chemistry. These advantages also come with potential limitations in computational cost. A more recent refinement of the LEM approach is the One-Dimensional Turbulence (ODT) model (Kerstein 1999a, b; Kerstein *et al.*, 2001). As stated by Kerstein *et al.* (2001) 'One-Dimensional Turbulence is a stochastic simulation method representing the time evolution of the velocity profile along a notional line of sight through a turbulent flow.'

LEM and ODT diverge in the manner the eddy size and rate distributions are implemented. In LEM, the frequency and the eddy size distribution of the stirring events are prescribed by a predefined kinetic energy spectrum (Kerstein, 1989). In ODT, one or more components of the velocity vector are transported. Therefore, the ODT model enables a mechanism for 'driving turbulence'. The frequency and the eddy size distribution are determined by the local flow field. In contrast with LEM, a mixing model, ODT is a self-contained turbulence model. The LEM and ODT models may be implemented as stand-alone models for turbulent flows where a dominant direction of the flow may be identified *a priori*. Such flows may constitute building blocks for more complex flows, and therefore provide useful validation of the ODT and LEM approaches. ODT has been implemented as a stand-alone model for homogeneous turbulent non-reacting (Kerstein, 1999a, b; Dreeben and Kerstein, 1998; Kerstein & Dreeben, 2000; Wunsch & Kerstein, 2001; Kerstein *et al.*, 2002; Ashurst *et al.*, 2003) and reacting flows (Echekki *et al.*, 2001, 2004; Hewson & Kerstein, 2001, 2002; Hewson *et al.*, 2002; Zhang & Echekki, 2005); however, more complex flows require the use of ODT and LEM within the framework of a three-dimensional flow solution approach such as LES.

Progress in implementing ODT within the context of LES for momentum transport has been achieved in the recent studies by Schmidt *et al.* (2003) and McDermott *et al.* (2005). Schmidt *et al.* (2003) implemented ODT within the context of a hybrid simulation with LES to model near-wall momentum transport, such that ODT solutions are extended from the bulk flow to the wall. The hybrid approach reproduces very well velocity profiles

normal to the wall, which are consistent with scaling rules in the inner region. The scheme by Schmidt *et al.* (2003) is also based on a two-way coupling between LES and ODT. McDermott *et al.* (2005) an algebraic stress model, denoted as the ensemble mean closure or EMC model, for closure of the subgrid stresses in LES based on the mappings and time scale physics used in ODT.

The objective of the present study is to develop a LES-ODT implementation for turbulent combustion. As outlined above, the need for a structure-based approach can address some of the key challenges arising in the prediction of non-linear physics on the subgrid scale. The implementation involves hybrid solutions of 3D LES with 1D ODT, with ODT domains or elements embedded within the LES computational domain. The solutions require the coupling of LES and ODT, the coupling of ODT elements, as well as the coupling of ODT "processes," which are implemented as combination of deterministic and stochastic implementations. A rigorous discussion of the numerical aspects of this coupling is beyond the scope of the present report. Such discussion, although important, warrants a separate manuscript. Instead, the present study focuses primarily on motivating the model development, a presentation of the numerical implementations, a discussion of key associated issues, and a validation of the LES-ODT model.

In the following sections, the basic elements of the LES-ODT model are presented (Sec. II) and key aspects of the numerical implementation are discussed (Sec. III). A numerical validation of the LES-ODT model based on the problem of autoignition in non-homogeneous mixtures is presented (Sec. IV), followed by a discussion of the results (Sec. V). Key observations on the performance of the LES-ODT model are reiterated in Sec. VI.

## II. THE LES-ODT STRATEGY

### A. Outline of the Proposed Strategy and Key Elements

Although the present validation effort has a limited scope, including a one-way coupling between LES and ODT, we will first introduce the LES-ODT model within the context of a fully-coupled hybrid scheme. The proposed LES-ODT formulation is based on two simulations that are implemented in the same volume (the computational domain). The first is a coarse-grained simulation based on the filtered transport equations for momentum and scalars (e.g. energy, species, and passive scalars). The second is based on fine-grained simulations implemented on an ensemble of ODT domains or elements that are embedded in the LES domain. These ODT elements are distributed in the computational domain in a similar manner to produce adequate statistics for filtered moments of scalars and derived quantities. In many respects, the LES-ODT approach is similar to the FDF approach. Both couple deterministic coarse-grained solutions with fine-grained solutions on representative elements in the computational domain. The added dimension provides mechanisms for estimating and coupling molecular process (reaction and diffusion) with turbulent transport, at least along the 1D domains of ODT. Moreover, this added dimension also enables the implementation of physical boundary conditions, such as walls. The distribution of the ODT elements is dictated by statistical requirements to capture needed closure terms; while, their orientation can be random or aligned to capture physical behavior more accurately.

## B. Model Formulation

The governing equations along the ODT elements are derived from the same equations governing the instantaneous vector and scalar fields of interest, and the same equations from which the filtered governing equations are derived; however, the resulting reduced equations on ODT elements will feature resolved contributions along the ODT domains, deterministic contributions from the filtered LES solution, and stochastic contributions from LES-unresolved transport terms. The formulation below describes a set of fixed ODT elements. We shall denote this formulation as the **Eulerian LES-ODT formulation**. We consider 3D unsteady fields for the three components of momentum and a set of scalars. At this stage of the formulation there are no assumptions about the molecular transport model, the chemical kinetics or the model for heat release. The scalars may correspond to measures of energy (e.g. temperature or internal energy), mixture composition (e.g. species mass fractions), and progress in chemistry, mixing, or phase change (e.g. reaction progress variable, mixture fraction). We present the scalar governing equations in terms of temperature and species mass fractions. The model involves the 3D solution of LES-filtered transport equations for total mass, momentum, and scalars and an equivalent set of one-dimensional ODT transport equations.

### *1. The Filtered Equations*

The LES governing equations are obtained by performing the filtering operation on the transport equations for scalars and momentum. These equations serve as the basis of LES-ODT model formulation and can be used for variable density as well as constant density flows. The equations are given as

***Continuity***:

$$\frac{\partial \bar{\rho}}{\partial t} + \frac{\partial \bar{\rho}\tilde{u}_i}{\partial x_i} = 0 \tag{1}$$

***Conservation of Momentum:***

$$\bar{\rho}\frac{\partial \tilde{u}_i}{\partial t} = \frac{\partial}{\partial x_j}\left[\bar{\rho}\left(\tilde{u}_i\tilde{u}_j - \widetilde{u_i u_j}\right)\right] + \left\{-\frac{\partial \bar{P}}{\partial x_i} - \bar{\rho}\tilde{u}_j\frac{\partial \tilde{u}_i}{\partial x_j} + \frac{\partial \bar{\tau}_{ij}}{\partial xj}\right\} \tag{2}$$

***Conservation of Energy:***

$$\bar{\rho}\frac{\partial \tilde{T}}{\partial t} = \overline{\frac{1}{c_p}\frac{\partial P}{\partial t}} - \overline{\frac{1}{c_p}\sum_{k=1}^{N} h_k\dot{\omega}_k} + \frac{\partial}{\partial x_i}\left[\bar{\rho}\left(\tilde{u}_i\tilde{T} - \widetilde{u_i T}\right)\right] + \left\{-\bar{\rho}\tilde{u}_i\frac{\partial \tilde{T}}{\partial x_i} + \frac{1}{c_p}\frac{\partial \bar{q}_i''}{\partial x_i}\right\} \tag{3}$$

***Conservation of Mass Fractions***

$$\rho\frac{\partial \tilde{Y}_k}{\partial t} = \bar{\dot{\omega}}_k + \frac{\partial}{\partial x_i}\left[\bar{\rho}\left(\tilde{u}_i\tilde{Y}_k - \widetilde{u_i Y_k}\right)\right] + \left\{-\bar{\rho}\tilde{u}_i\frac{\partial \tilde{Y}_k}{\partial x_i} + \frac{\partial \bar{J}_{k,i}}{\partial x_i}\right\} \tag{4}$$

In the above equations, the dependent variables, $\rho$, $u_i$, $T$ and $Y_k$, represent the mass density, the $i$th component of the velocity vector, the mixture temperature, and the $k$th species mass fraction, respectively. Other symbols in the governing equations include the pressure, $P$, the heat flux in

the $i$th direction, $\dot{q}_i''$, the mixture heat capacity, $c_p$, the $k$th species total enthalpy, $h_k$, and the its corresponding production rate, $\dot{\omega}_k$. In Eq. (2), the viscous stress tensor, $\tau_{ij}$, is expressed in terms of the dynamic viscosity, $\mu$, and the strain rate tensor, $S_{ij}$, as follows:

$$\tau_{ij} = 2\mu S_{ij} \text{ where } S_{ij} = \frac{1}{2}\left(\frac{\partial u_i}{\partial x_j} + \frac{\partial u_j}{\partial x_i}\right) - \frac{1}{3}\delta_{ij}\frac{\partial u_k}{\partial x_k} \tag{5}$$

In Eq. (4), $\bar{J}_{k,i}$ is the diffusive flux of species $k$ in direction $j$, $\bar{J}_{k,i}$. The symbol '$-$' corresponds to the implementation of a spatial filter function, $G$, such that a filtered quantity, $\phi$, defined at a spatial position, $x$, and time, $t$, is expressed as: $\bar{\phi}(\mathbf{x},t) = \iiint_{\Delta} \phi(\mathbf{x}',t)\cdot G(\mathbf{x}-\mathbf{x}',\Delta)\,d\mathbf{x}'$. The symbol '$\sim$' in Eqs. (1)–(4) corresponds to a Favre-averaged filtering of a given quantity, $\phi = \tilde{\phi} + \phi^*$, where $\tilde{\phi}$ and $\phi^*$ represent the resolved and unresolved contributions to the variable $\phi$ in the LES solution, respectively. The terms $\left(\widetilde{u_i u_j} - \widetilde{u_i}\,\widetilde{u_j}\right)$ in Eq. (2) are the subgrid stresses. Terms $\left(\widetilde{u_i T} - \widetilde{u_i}\,\widetilde{T}\right)$ in Eq. (3) and $\left(\widetilde{u_i Y_k} - \widetilde{u_i}\,\widetilde{Y_k}\right)$ in Eq. (4) are subgrid fluxes for temperature and species, respectively. Those subgrid stresses and fluxes need to be modeled using a subgrid closure model.

## 2. The ODT Governing Equations

On each ODT element, a set of momentum and scalar equations is derived. These equations feature both resolved contributions on the 1D ODT domains and unresolved contributions. These equations also are represented in terms of a hybrid scheme with deterministic and stochastic contributions. The coordinate system on which the governing equations are based is Cartesian with one component along the ODT domain, $\eta$, and two additional orthogonal components, $x_1$ and $x_2$. In the simplest layout of the ODT domain topology, a Cartesian lattice of ODT elements may be adopted as shown in Fig. 1.

A principal element of the coupling of a coarse-grained simulation approach (LES) with a fine-grained approach is the representation of turbulent transport for momentum and scalars below the LES resolution. Different interpretations of resolution may evolve from the use of implicit filtering (Schumann) or explicit filtering of the LES governing equations (1)-(4). In principle, both approaches can be implemented with the context of the LES-ODT approach. To represent LES-unresolved transport, we decompose the velocity field into 'resolved' and 'unresolved' components:

$$u_i = \tilde{u}_i + u_i^*. \tag{6}$$

Here, we assume that while the LES-solution for the velocity vector is evaluated numerically on a discrete coarse-grid, it is possible to interpolate it onto a finer grid, while maintaining a reasonable separation between LES-resolved and LES-unresolved scales. The second component of the velocity decomposition, $u_i^*$, represents the unresolved component in LES, which is represented by the turbulent stirring events in ODT. The governing equations on each ODT element of momentum, temperature, and species mass fractions are:

***Conservation of Momentum***

$$\frac{\partial u_i}{\partial t} = \left[\frac{1}{\rho}\frac{\partial \tau_{i\eta}}{\partial \eta} + \Omega_{u_i}\right] + \left\{-\frac{1}{\rho}\frac{\partial P}{\partial x_i} - \tilde{u}_j\frac{\partial u_i}{\partial x_j} + \frac{1}{\rho}\left(\frac{\partial \tau_{i1}}{\partial x_1} + \frac{\partial \tau_{i2}}{\partial x_2}\right)\right\} \tag{7}$$

***Conservation of Energy***

$$\frac{\partial T}{\partial t} = \left[\frac{1}{\rho c_p}\frac{\partial P}{\partial t} + \frac{1}{\rho c_p}\frac{\partial \dot{q}''_\eta}{\partial \eta} - \frac{1}{\rho c_p}\sum_{k=1}^{N} h_k \dot{\omega}_k + \Omega_T\right] + \left\{-\tilde{u}_i\frac{\partial T}{\partial x_i} + \frac{1}{\rho c_p}\left(\frac{\partial \dot{q}''_1}{\partial x_1} + \frac{\partial \dot{q}''_2}{\partial x_2}\right)\right\} \tag{8}$$

***Conservation of Mass Fractions***

$$\frac{\partial Y_k}{\partial t} = \left[\frac{1}{\rho}\frac{\partial J_{k,\eta}}{\partial \eta} + \frac{\dot{\omega}_k}{\rho} + \Omega_{Y_k}\right] + \left\{-\tilde{u}_i\frac{\partial Y_k}{\partial x_i} + \frac{1}{\rho}\left(\frac{\partial J_{k,1}}{\partial x_1} + \frac{\partial J_{k,2}}{\partial x_2}\right)\right\} \tag{9}$$

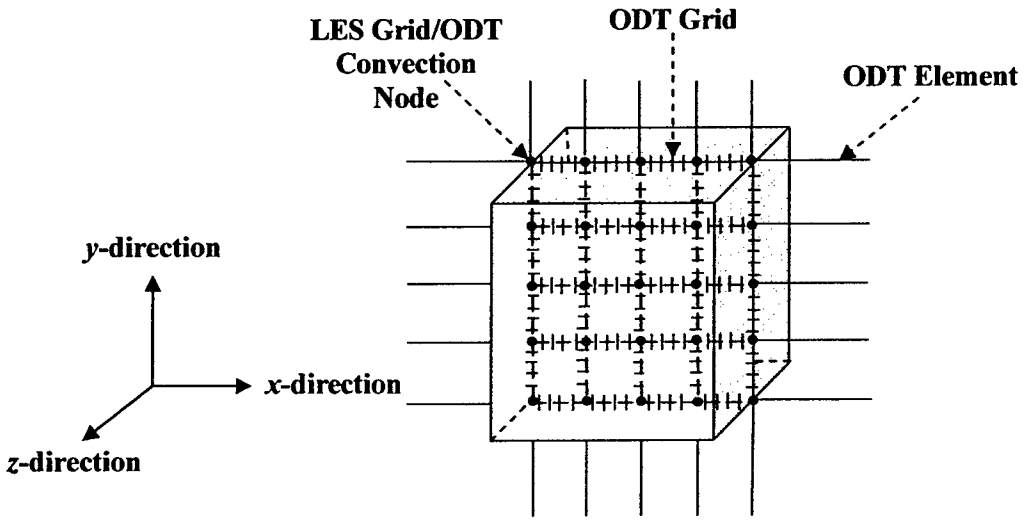


**Figure 1.** Schematic layout of the ODT elements in *x*-*y* plane based on an ODT lattice configuration.

In the above equations, the ODT governing equations feature contributions that are resolved on the ODT domain and other contributions that require gradients along the normal components to the ODT domain. The resolved contributions include: (1) molecular transport with gradients along the 1D domain, (2) chemical source terms, and (3) the stochastic contributions, $\Omega_{u_i}$, $\Omega_T$, and $\Omega_{Y_k}$. The stochastic contributions represent 3D transport events, including stirring, pressure scrambling, and contributions from fluctuating terms in the different variables. The stochastic contributions are implemented as instantaneous stirring events through triplet maps (Kerstein 1999a).

The 'triplet map' is illustrated in Fig. 2. Given a selected eddy size defined by its length, $l$, and its starting point, $y_0$, on the 1D domain the triplet map converts an initial field of a dependent variable (e.g. scalar composition) $\varphi(y)$ to $\varphi(m(y))$ where:

$$m(y)=\begin{cases} 3(y-y_0), \text{ if } y_0 \le y \le y_0+\dfrac{l}{3} \\ 2l-3(y-y_0), \text{ if } y_0+\dfrac{l}{3} \le y \le y_0+\dfrac{2l}{3} \\ 3(y-y_0)-2l, \text{ if } y_0+\dfrac{3l}{3} \le y \le y_0+l \\ y-y_0, \text{ otherwise} \end{cases} \tag{10}$$

The triplet map also translates into a displacement of the dependent variable $\varphi(y)$ (McDermott *et al.*, 2005):

$$\Psi(y;y_0,l)=\int_y^{y_0+l}[\varphi(m(\eta))-\varphi(\eta)]d\eta\,. \tag{11}$$

The resulting flux rate corresponding to a discrete set of stirring events at a given position, $y$, over a period $\Delta t$, is expressed as:

$$F_\varphi(y)=\frac{1}{\Delta t}\sum_m \varphi^m\left(y;y_0^m,l^m\right) \tag{12}$$

where the superscript $m$ corresponds to one of the discrete stirring events. McDermott *et al.*. (2005) show that, under simplifying assumptions, the ODT stirring can yield similar scaling of SGS stresses with resolved strain to the model derived using the basic Smagorinsky model, and its underlying assumptions. Earlier analysis by Kerstein (1992) showed that the transport induced by turbulent stirring events can be interpreted in terms of a turbulent diffusivity. Kerstein used his analysis to derive expressions for the eddy-size distribution and the eddy rate frequency within the context of LEM and based on a prescribed kinetic energy spectrum.

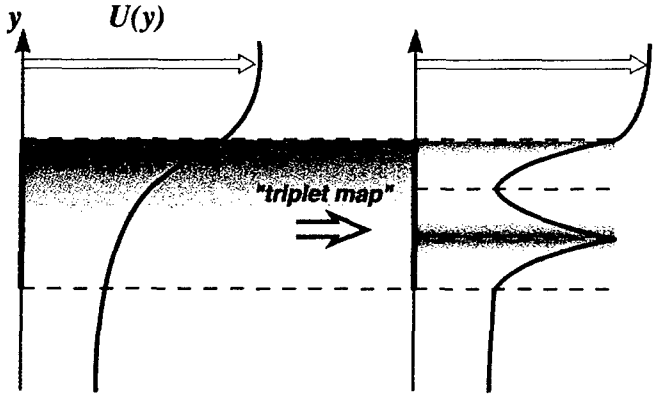


**Figure 2.** Implementation of a triple map on a segment in the ODT profile. The triplet map is a conservative rearrangement event that consists of the replacement of 1D profile on the selected segment by three identical copies compressed to one-third of their original size, with the middle copy inverted. The triplet map results in the tripling of gradients and interfaces within that segment.

Another important implementation detail concerns the implementation of ODT-unresolved contributions due to filtered advective and diffusive fluxes. The implementation of filtered advective fluxes in the present work represents one of the more significant contributions of the present effort.

## *4. General Comments*

While an LES-ODT approach can be promoted for momentum closure, which constitutes an integral part of the validation of the model in this research effort, the true advantage of the approach is its potential to capture the statistics of processes that originate in the subgrid scale. Concerns about capturing these statistics are common among many turbulent mixing and turbulent combustion problems. The model has a number of attractive features:

(1) The LES-ODT approach is a statistical approach given the stochastic contributions from ODT and its one-dimensional nature. Therefore, the predictions of LES-ODT models are primarily of value at the LES time and length scales.

(2) The LES-ODT governing equations contain redundancies, which can be used to fine-tune model constants or evaluate closure terms based on ODT of subgrid scale stresses or fluxes or source terms. We denote this approach as a two-way coupling of the LES and ODT solutions (Schmidt *et al.*, 2003). The presence of redundancies also means that potentially we can rely on one particular component of the model, say LES or ODT, to resolve a given quantity. We denote this approach as one-way coupling. This approach is adopted for the present validation study.

(3) The ODT governing equations are derived in physical space, albeit in 1D. Physical boundary conditions, such as walls or interfaces with other phases can be applied in a more transparent way than particle-based (e.g. FDF approaches) or phase-space based formulations.

(4) In contrast with LES-LEM, the LES-ODT model may be used to 'close' both momentum and scalar terms in the LES-filtered equations and to implement a more robust coupling between momentum and scalar transport equations. More importantly, since ODT is a turbulence model, there is no implicit assumption about the mechanism or associated statistics of the turbulence conditions used. For example, an ODT implementation can adapt to transitions from an inertia-driven flow to a buoyancy-driven flow, such as in jets.

(5) In contrast with phase-space models, such as the flamelet approach or the conditional moment closure (CMC) model (Peters, 2000), there is no implicit assumption about the combustion model, regime, or dominant chemistry required to reduce the parameter space based on these models. The ability to capture physics without these restrictions is an attribute that LES-ODT shares with FDF approaches as well as the LES-LEM approach.

(6) The ODT governing equations couple contributions from molecular transport, chemical source terms and advection within a single 1D domain. Therefore, the LES-ODT formulation remains true to its original principle of coupling molecular and turbulent transport processes along the entire range of scales. Moreover, mixing in the ODT model is local in both physical and wave spaces, allowing for a more realistic representation of transport and the kinetic energy cascade in turbulent flows. Turbulent advection on the 1D domains is implemented stochastically with mapping events, each involving the application of a "triplet map" to a randomly selected segment (eddy). Despite its simplicity, the triplet map was shown to reproduce traditional Kolmogorov inertial and dissipative scaling, Batchelor's Prandtl number dependent passive-scalar subrange scaling, and the Bolgiano-Obukhov scaling of buoyancy-driven scalar spectra (Kerstein, 1999a, 1999b).

(7) With spatially and temporally resolved solutions of momentum and scalar variables, variances and co-variances of joint velocity and scalars, as well as two-point statistics, can be constructed based on ODT solutions.

## III. NUMERICAL IMPLEMENTATION

We have outlined above a general framework for the formulation of an LES-ODT model for turbulent combustion. In reality, additional equations may be swapped with the energy and species equations to address other physics. We also have pointed out potential redundancies in the governing equations that may yield different ways of coupling LES and ODT solutions. In this section, we discuss implementation issues and address key implementation details based on the LES-ODT model that is adopted for the present validation. The numerical solution of the LES-ODT transport equations is obtained using a finite-difference scheme for the LES-filtered equations and a hybrid finite-difference and Monte-Carlo procedure for the ODT equations. The different contributions representing the terms on the right-hand side of the ODT governing equations are treated as parallel processes based on a split operator scheme. These processes include (1) reaction-diffusion terms, (2) stochastic stirring events, and (3) advection terms. Additional processes involving the collection of statistics also can be implemented within the context of the ODT solutions.

The ODT solutions are implemented on an ensemble of ODT domains, or elements, that are embedded in the LES domain. In their simplest form, the ODT elements are distributed on an orthogonal lattice representing the principal components of a Cartesian coordinate system (see Fig. 1). In a more general form, the ODT elements are allowed to be advected with a characteristic velocity (such as the filtered velocity) and rotated by the velocity field to assume arbitrary orientations with respect to the LES grid. Additional considerations for the hybrid LES-ODT solutions involve the temporal and spatial coupling of these solutions. Below we discuss in general terms the proposed approaches for the integration of the various terms. In the validation section, we provide more specific implementation details adopted for the validation study.

In the present model validation study, the LES-filtered momentum equations are resolved using the standard Smagorinsky model for the SGS stresses. No scalar equations are transported, and therefore, in the absence of heat release, there is no feedback coupling from the ODT solutions to the LES solutions. There is, however, coupling that is carried out to establish consistency between the momentum equations in LES and ODT. Moreover, as shown below, the LES solution for the momentum equations is filtered inversely onto the ODT solutions to implement the proposed advection scheme.

### A. Molecular processes

Molecular processes in the ODT governing equations include (1) reaction, (2) diffusion along the ODT elements' directions, and (3) diffusion along the directions normal to the ODT elements. While the first and second contributions can be resolved exactly on the ODT grid, the third contribution must be modeled. In principle, different strategies can be adopted to model this contribution. These include:

1. A flame-normal approach in which ODT elements are aligned with the dominant direction of scalar gradients, such that on average, these gradients are captured with a 1D description. These gradients may indicate the presence of a flame 'brush'. However, within the context of LES, the direction of the gradients will evolve in time; therefore, a flame-normal approach can be reasonably addressed primarily through a Lagrangian description of ODT.
2. The use of the filtered solution of scalar gradients in the three principal directions. However, important considerations of scalar boundedness must be addressed when coupling LES-resolved terms on the LES time step and ODT solutions. Moreover, diffusion is inherently coupled with reaction, and the introduction of filtered contributions may significantly alter this coupling.
3. The representation of non-resolved diffusive contributions through an enhanced diffusion in one dimension along the ODT elements. This may be achieved through a local isotropic prescription of scalar gradients. This corresponds to an enhancement of the rate of diffusion by a factor of 3. A possible refinement to this approach is to identify an alternative factor based on the ratios of the LES-filtered diffusive fluxes or scalar gradients. In the present validation study, we adopt the simpler approach. The reaction-diffusion operators in the governing equations are modeled as: $(\rho \partial u_i/\partial t)^{\mathrm{MOL}} = 3\,\partial/\partial\eta(\mu\ \partial u_i/\partial\eta)$, $(\rho \partial T/\partial t)^{\mathrm{MOL}} = (1/c_p)\partial P/\partial t + (3/c_p)\,\partial \dot{q}''_\eta/\partial\eta - (1/c_p)\sum_{k=1}^{N} h_k \dot{\omega}_k$, and $(\rho \partial Y_k/\partial t)^{\mathrm{MOL}} = 3\,\partial J_{k,\eta}/\partial\eta + \dot{\omega}_k$. The superscript 'MOL' refers to the molecular contribution to the governing equations. The other terms in the expressions for the reaction-diffusion operators have the same meaning as described earlier.

The choice of the integration scheme for these operators may be largely dictated by the stiffness and complexity of the chemical mechanism. Further splitting of the diffusion and reaction terms may be computationally efficient as implemented in the study of Echekki *et al.* (2001).

## B. Stirring Processes

Stirring events are implemented as discrete events dictated by a sampling frequency for stirring. During a stirring event an eddy size and location are sampled randomly out of the available length scales and positions within the domain. Subject to rules of stirring, a stirring event is implemented by locally implementing a triplet map on profiles of velocity components and scalars covering the extent of the eddy. Stirring events are implemented using the rules dictated by the recent formulation of ODT, the vector formulation (Kerstein *et al.*, 2001). The formulation includes the solution for a three-component velocity field on the 1D ODT elements along with any number of scalar transport equations. The formulation, in particular, enables inter-component energy transfer based on the return-to-isotropy concept; therefore, in contrast with the original ODT formulation (Kerstein, 1999), stirring events involve the application of a triplet map and a redistribution of kinetic energy among the three components of the velocity. A parameter, $\alpha$, in the model regulates the extent of the energy transfer, with a maximum value corresponding to $\alpha = 1$. The implementation of the triplet map may be limiting the upper range to which the LES filter may be extended fundamentally.

The time sequence of stirring events, which are implemented on individual eddies, is prescribed by an event rate distribution. This rate distribution is evaluated by associating a characteristic length and time scale to the selected eddy. The time scale is analogous to an eddy turnover time; and is therefore expressed in terms of the eddy size and characteristic velocities (or kinetic energies), computed based on a weighted average on the eddy. The primary ODT model constant, $C$, is of order unity and relates the actual rate distribution and the theoretical rate distribution. An additional viscous penalty constant, $c_Z$, is used in adjusting the characteristic kinetic energy in the eddy with the rate of dissipation associated with that eddy. An additional model parameter is the maximum size of eddies, $L_{max}$, which is dictated by the Nyquist limit, the smallest eddy that can be represented on the LES grid. Additional details of the implementation of stirring events are found in Kerstein *et al.* (2001).

## C. Advection

A principal innovation of the present study is the treatment of the filtered advection of momentum and scalars in ODT, which are represented by the operators: $(\partial u_i/\partial t)^{ADV} = -\tilde{u}_j\, \partial u_i/\partial x_j$, $(\partial T/\partial t)^{ADV} = -\tilde{u}_j\, \partial T/\partial x_j$ and $(\partial Y_k/\partial t)^{ADV} = -\tilde{u}_j\, \partial Y_k/\partial x_j$ in the ODT governing equations. The implementation of filtered advection represents a fundamental challenge for the following reasons:

(1) Advective transport is a 3D process; thus, at least two directions are not resolved on the ODT time scale or on the ODT 1D elements. A principal challenge is to represent unresolved contributions to advection, at least statistically.

(2) Non-linear contributions from advection processes pose important constraints on scalar boundedness. Scalar boundedness is an important problem in the solution of combustion flows that is made critical by the presence of both ODT resolved and LES resolved terms within the advection operator. Scalar boundedness problems also are critical for problems involving the solution of both major and minor species of combustion.

The representation of gradients and advective fluxes along the principal directions of transport is a critical component of the present model. These fluxes may be constructed exactly along "nodes" that represent the intersection in space of three or more ODT domains. Along these nodes, the solution of the velocity and scalar equations are updated; then, ODT solutions between these nodes are updated through a single component advection along the corresponding ODT element. In a Cartesian lattice of ODT elements, these nodes represent the intersection of three orthogonal 1D domains. Below, we will describe the implementation based on this Cartesian lattice configuration. The filtered advection process as implemented as a separate process concurrently with reaction-diffusion and stirring processes. The treatment of three-dimensional fluxes within ODT solutions is implemented through a two-step process: (1) node advection, and (2) intra-node relaxation:

- **Node Advection:** At the prescribed time step for filtered advection, the solution at each node is evaluated based on gradients represented by the 3 ODT elements intersecting at the node. This step is implemented as follows:

(a) The three components of the advective flux are evaluated through the separate contributions from these ODT elements.

(b) These components added to represent the overall contribution to advection operators, $-\tilde{u}_j \partial u_i/\partial x_j$, $-\tilde{u}_j \partial T/\partial x_j$ and $-\tilde{u}_j \partial Y_k/\partial x_j$.

(c) The solution at the nodes is updated based on the combined fluxes and the advection operators alone.

At the end of this process, the updated node solution is reflected in all contributing 3 ODT elements. The governing principle for the proposed node advection strategy is to channel advective fluxes through ODT nodes is a similar strategy to what has been adopted for Lattice Gas (LG) and Lattice-Boltzmann (LB) methods. These two methods rely on the description of macro-scale fluid transport in terms of discrete particles moving along a lattice.

- **Intra-node Relaxation:** At the end of the node advection step, the solution is updated at the ODT nodes. The second step involves an update, or a relaxation, of the solution between these nodes, while the solution at the nodes is fixed. This is achieved through the integration of the solution in between the nodes using single-component advective fluxes according to the following relations: $(\partial u_i/\partial t) = -\kappa\, \tilde{u}_\eta\, \partial u_i/\partial \eta$, $(\partial T/\partial t) = -\kappa\, \tilde{u}_\eta\, \partial T/\partial \eta$ and $(\partial Y_k/\partial t) = -\kappa\, \tilde{u}_\eta\, \partial Y_k/\partial \eta$. In these relations, $\kappa$ is a relaxation coefficient, which governs the rate at which the intra-node solution is updated to reflect changes at the nodes. Because the LES-ODT approach is inherently a statistical approach, there exists a reasonable range for the values of $\kappa$ that can still yield reasonable predictions of the scalar and momentum statistics on the LES time scale. It is equally possible to implement intra-node relaxation in terms of successive implementations (or cycling) a number of times between each node advection event. Presently, the trade-offs between enhancing the coefficient, $\kappa$, or cycling intra-node advection has not been fully investigated. The use of advection fluxes along the ODT elements manages the "flow" of statistics from the nodes, which is largely governed by the rate of transport and determines the relative contribution of the surrounding nodes.

The implementation of a flux-limiting scheme is an important aspect of the numerical implementation of filtered advection for the above steps. In the validation study presented below, we use a total variation diminishing (TVD) scheme with a flux limiter, based on the "Superbee" limiter of Roe (Tannehill, 1997) to enforce scalar boundedness. Other strategies to address higher order schemes or different constraints to the overall numerical solution can be adopted as well (Oran and Boris, 2001).

## D. Coupling of LES and ODT Solutions

The coupling of LES and ODT solutions is implemented both temporally and spatially. The LES and ODT solutions are coupled at each LES time step as shown schematically in Fig. 3. The solution scheme involves an ODT integration of the various concurrent sub-steps, for molecular processes, stirring, advection and statistics, up to a LES time-step. In practice, a multi-step LES numerical procedure (e.g. predictor-corrector approach) may lend itself more readily for coupling LES with ODT. Such a procedure may be provided to refine variables that are transmitted from one solution approach to another. In Fig. 3, the

LES time-steps is shown shifted by half an ODT integral time step to accurately represent these variables within the two schemes.

During the temporal integration of the two solutions, statistics are transmitted from one solution scheme to another. For ODT, the LES-filtered velocity field, $\tilde{\mathbf{u}}$, may be evaluated from the LES solution of the momentum equations. For LES, a number of variables may be obtained from ODT, including closure for the mass density, $\bar{\rho}$, SGS stresses and fluxes, $\left(\widetilde{u_i u_j} - \tilde{u}_i \tilde{u}_j\right)$, $\left(\widetilde{u_i T} - \tilde{u}_i \tilde{T}\right)$ and $\left(\widetilde{u_i Y_k} - \tilde{u}_i \tilde{Y}_k\right)$, or filtered sources terms, $\overline{\frac{1}{c_p}\sum_{k=1}^{N} h_k \dot{\omega}_k}$ and $\overline{\dot{\omega}_k}$. Diffusive fluxes or diffusion coefficients may also be evaluated through filtering of the ODT solutions. In reality, the degree of coupling may be dependent on the actual transport equations solved in the LES filtered equations, the type of closure needed in these equations, and the assumptions of the model. For example, in the present validation study, only the LES momentum equations are solved. The LES and ODT solutions are made consistent by adjusting the ODT velocity field at the end of an integral time step. This adjustment is achieved by adding a 'correction' to the ODT velocity components, such that residual terms are maintained, and the filtered contribution corresponds to the LES-filtered velocity field, $\tilde{\mathbf{u}}$:

$$u_{i,\mathrm{ODT}} \rightarrow \tilde{u}_{i,\mathrm{LES}} + u^{*}_{i,\mathrm{ODT}}, \text{ where } u^{*}_{i,\mathrm{ODT}} = u_{i,\mathrm{ODT}} - \tilde{u}_{i,\mathrm{ODT}}. \tag{13}$$

Note that the velocity components $\tilde{u}_{i,\mathrm{ODT}}$ and $\tilde{u}_{i,\mathrm{LES}}$ correspond to $i$th component of the ODT filtered velocity components based on the ODT solutions and the LES-resolved velocity components based on the LES governing equations, respectively. The adjustment of ODT velocity field enforces the consistency of the velocity fields between LES and ODT. Because the adjustment is made at regular LES time-step intervals, the pressure correction term is not explicitly implemented in the node-advection scheme discussed above. Instead, pressure correction is implemented implicitly within the velocity adjustment in Eq. (13).

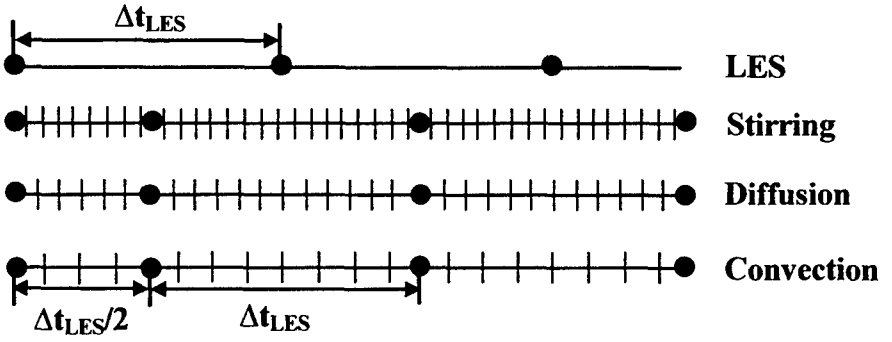


**Figure 3.** Coupling of LES and ODT.

## IV. APPLICATION: NON-HOMOGENEOUS AUTOIGNITION

Using the formulation presented above, we simulate autoignition in non-homogeneous mixtures. An attempt to capture this complex physics is a challenge for state-of-the-art models in turbulent combustion. In a non-homogeneous mixture, the rate of chemistry competes with the rates of turbulent mixing and diffusion, resulting in different autoignition regimes. The details of this competition eventually determine the volumetric rates of heat release, the fate of the reacting mixture and the evolution of the reactive scalars statistics. During this process, the dominant chemical reactions, the mode of combustion (e.g. premixed, non-premixed) or the combustion regime (e.g. flamelet, distributed reaction) may evolve in time. Autoignition in non-homogeneous mixture is initiated at discrete autoignition sites where the local conditions for the onset of chemistry are favorable (e.g. low dissipation rate, favorable temperature and mixture composition). More importantly, these sites can be initially small, and far below the resolution of the LES grid.

## A. DNS Simulation of Non-Homogeneous Autoignition

To evaluate the LES-ODT model predictions, Direct Numerical Simulations (DNS) of the same problem are implemented. The initial mixture is prescribed as a random field of mixture strengths separating "islands" of fuel and oxidizer, where the oxidizer is heated relative to the fuel. The main flow assumptions used here include ideal gas behavior, constant density, constant transport coefficients, and negligible radiation, Soret, and Dufour effects. Although the formulation below can be easily extended to variable density conditions, we have made the constant density assumption to establish the same evolution of turbulence conditions in the cases considered for the same initial flow conditions. With a variable-density assumption, the filtered density field may be evaluated using ODT solutions and provided for closure of the LES governing equations. We also assume that all species have the same constant mass diffusivity. The resulting non-dimensional governing equations are:

- Continuity

$$\frac{\partial u_i}{\partial x_i} = 0, \tag{14}$$

- Momentum

$$\frac{\partial u_i}{\partial t} + u_j \frac{\partial u_i}{\partial x_j} = -\frac{1}{\rho}\frac{\partial p}{\partial x_i} + \nu \frac{\partial^2 u_i}{\partial x_j^2}, \tag{15}$$

- Temperature

$$\frac{\partial T}{\partial t} + u_j \frac{\partial T}{\partial x_j} = \frac{\nu}{Pr}\frac{\partial^2 T}{\partial x_j^2} + Q\hat{\omega}, \tag{16}$$

- Species (fuel and oxidizer mass fractions)

$$\frac{\partial Y_{F,O}}{\partial t} + u_j \frac{\partial Y_{F,O}}{\partial x_j} = \frac{\nu}{Pr\,Le}\frac{\partial^2 Y_{F,O}}{\partial x_j^2} - \hat{\omega}. \tag{17}$$

In the above equations, the subscripts "F" and "O" refer to the fuel and the oxidizer, respectively; while the other symbols and subscripts carry their usual meaning. The non-dimensional parameters, *Pr* and *Le*, correspond to the Prandtl number and the Lewis number for all species, including the fuel (F), the oxidizer (O) and the product (P), respectively. The kinematic viscosity, $\nu$, in a normalized form can be written as an inverse of a Reynolds number, $Re = 1/\nu$. The value of this Reynolds number is based on the magnitude of the kinematic viscosity and the characteristic length and velocity scales used to normalize the various physical quantities. As written in the governing equations, the Lewis number is the same for all species, and, therefore, it measures the relative rates of heat diffusion to mass diffusion for these species.

The reaction rate of the fuel and oxidizer and the rate of heat release are prescribed by the single-step, second-order, irreversible reaction of the fuel, F, with the oxidizer, O:

$$\mathrm{F} + \mathrm{O} \rightarrow \mathrm{P}. \tag{18}$$

The rate of progress of reaction is expressed in Arrhenius form as follows:

$$\hat{\omega} = \frac{B}{W}\rho^2 Y_F Y_O \exp\left(\frac{-E_a}{R_u T}\right), \tag{19}$$

where the individual rates of production and consumption of products and reactants are related as follows: $\hat{\omega} = -\omega_F = -\omega_O$. In this expression, F, O and P and associated subscripts refer to the fuel, oxidizer, and product respectively. The rates constant parameters, $B$ and $E_a$, correspond to the pre-exponential frequency factor and the activation energy, respectively. The constant, $R_u$, is the universal gas constant. We further assume that all species have the same molecular weight, $W$, such that at stoichiometric conditions, the fuel and oxidizer mass fractions are 0.5. At any time of the computation, the mixture fraction, $Z$, is prescribed as follows:

$$Z = \tfrac{1}{2}\left(1 + Y_F - Y_O\right). \tag{20}$$

The mixture fraction is used to evaluate conditional statistics of reactive scalars based on this quantity. The low Mach number approximation is used to solve the transport equations. The DNS code is based on the formulation by Mason (2000). The same code has been generalized to compute the LES equations in LES-ODT, and is coupled with the ODT solver. Non-staggered uniform grids are used in the formulation. A third-order Runge-Kutta method is used to integrate the system of equations in time. A fully consistent fractional-step method is used for the solution of the momentum equation. The pressure in the momentum equation is solved using the Poisson's equation. Linearly implicit variation of third-order Runge-Kutta scheme is used to integrate the energy and the species equations. Spatial derivatives are computed using the fifth-order explicit finite-difference schemes.

## B. LES-ODT Simulation of Non-Homogeneous Autoignition

### *1. Governing Equations*

The governing equations are:

- LES continuity

$$\frac{\partial \bar{u}_j}{\partial x_j} = 0, \tag{21}$$

- LES momentum ($i = 1, 2, 3$)

$$\frac{\partial \bar{u}_i}{\partial t} + \bar{u}_j \frac{\partial \bar{u}_i}{\partial x_j} = -\frac{1}{\rho}\frac{\partial \bar{p}}{\partial x_i} + (\nu + \nu_T)\frac{\partial^2 \bar{u}_i}{\partial x_j^2}. \tag{22}$$

The turbulent viscosity, $\nu_T$, is expressed based on the Smagorinsky model as:

$$\nu_T = (C_S \Delta)^2 \left(2 \bar{S}_{ij} \bar{S}_{ij}\right)^{1/2}, \tag{23}$$

where $\bar{S}_{ij}$ is the filtered rate of strain, which may be evaluated from the LES-resolved solution of the velocity vector. The constant $C_S$ is the Smagorinsky constant, and the length scale, $\Delta$, is the characteristic filter width. In the present computations, it is taken as the grid size, which is uniform and is the same in each direction. The ODT governing equations are:

- ODT Momentum ($i = 1, 2, 3$)

$$\frac{\partial u_i}{\partial t} = 3\nu \frac{\partial^2 u_i}{\partial \eta^2} + \Omega_{u_i} - \tilde{u}_j \frac{\partial u_i}{\partial x_j}, \tag{24}$$

- ODT Energy

$$\frac{\partial T}{\partial t} = \left(3\frac{\nu}{Pr}\frac{\partial^2 T}{\partial \eta^2} + Q\hat{\omega}\right) + \Omega_T - \tilde{u}_j \frac{\partial T}{\partial x_i}, \tag{25}$$

- ODT Species (fuel and oxidizer)

$$\frac{\partial Y_{F,O}}{\partial t} = \left(3\frac{\nu}{Pr\,Le}\frac{\partial^2 Y_{F,O}}{\partial \eta^2} - \hat{\omega}\right) + \Omega_{Y_{F,O}} - \tilde{u}_j \frac{\partial Y_{F,O}}{\partial x_j}. \tag{26}$$

In the above equations, the terms inside the brackets '( )' on the right-hand side represent the deterministic reaction-diffusion operators. The second terms on the right-hand side represent the stochastic stirring events; and the last terms represent filtered advection.

## 2. Initial and Boundary Conditions

The initial field in the DNS simulation is prescribed with a von Karman-Pao spectrum (Hinze, 1975) for the mixture fraction fluctuation correlation function. The mixture fraction represents a normalized measure of the mixture composition, such that it is zero on the oxidizer side of the mixture and unity on its fuel side. Fig. 4 shows isosurfaces of the initial mixture fraction field indicating the spatial distribution of the mixture strength from lean to rich conditions. The same form of the spectrum is also used to prescribe the initial kinetic energy spectrum. The DNS initial conditions are prescribed consistently with the LES-ODT computation. The initial field velocity and scalar fields from DNS are interpolated to the ODT elements using tri-linear interpolation. The initial LES flow field is obtained by filtering the ODT flow field using the box filter. Periodic boundary conditions are imposed in all three directions for both DNS and LES-ODT simulations. Periodic boundary

conditions along ODT elements are also implemented for stirring events extending beyond one element physical boundary.

## 3. Run Conditions and Model Parameters

The following parameters are prescribed for all DNS and LES-ODT cases considered, $Pr$ = 0.7, $Re$ = 200, $Da$ = 200, and $\beta$ = 2. The heat release parameter, $\alpha_0$, which is the ratio of the temperature difference between products and reactants to the products temperature at stoichiometric conditions, is chosen as 0.75. This value indicates a temperature ratio between reactants and products of 4 at stoichiometric conditions. The Lewis numbers are set differently for the different cases considered.

The ODT model constants $\alpha$, $C$, and $C_z$ are chosen to be consistent with the values adopted by Kerstein *et al.* (2001). They correspond to a value of $\alpha$ = 2/3, $C$ = 3.78, and $C_z$ = 0.04. No additional fine-tuning of these parameters is implemented here. A future extension of the present effort is to explore optimum static values for these parameters or methods to determine them dynamically. The model constant $L_{max}$ may be prescribed as a factor of the LES grid, $\Delta$; and we have adopted a value of the ratio, $L_{max}/\Delta$ = 2; this is a reasonable choice, as it corresponds approximately to the factor associated with Nyquist limit. The value of Lmax is found to yield reasonable results in the recent near-wall LES-ODT simulations by Schmidt *et al.* (2003). The coefficient $\kappa$ for intra-node relaxation is set to unity. Additional enhancements of this coefficients or the implementation of cycling between node advection events only yields marginal improvements on the LES-ODT reactive scalars' statistics.

The simulations are based on four different conditions that represent two distinct turbulent flow conditions and different Lewis number values at the higher turbulence conditions. The different conditions are chosen to highlight the roles of turbulent and molecular transport on the transient evolution of the autoignition process. The base case corresponds to the lower turbulence conditions at Taylor scale Reynolds number of 100 and a unity Lewis number for all species considered. The turbulence intensity for this case normalized by the characteristic velocity is 0.74. The other conditions correspond to a Taylor scale of 405, and a corresponding normalized turbulence intensity of 3.0. Three different Lewis numbers are used for this high turbulence condition, including 0.5, 1 and 2. Despite these differences, the different cases considered share the following initial conditions:

(1) The initial mixture fraction distribution is identical to identify the role of transport in mixing and chemistry.

(2) Both low-turbulence and high-turbulence conditions have the same structure in both physical and spectral spaces. The high-turbulence initial velocity field corresponds point-by-point on the computational domain to a factor of 3.0/0.74 the corresponding value for the low-turbulence case. This choice of initialization enables the identification of the role of turbulence intensity.

The computational domain size is 4.2 in each direction. The corresponding DNS resolution is $129^3$. Two different resolutions are computed with LES. They are denoted as case A and case B in the simulations, and correspond to a resolution $9^3$ and $17^3$, respectively. Figure 5 shows a profile of the kinetic energy spectrum as a function of the wave number based on the DNS initial velocity profiles of both the high-turbulence and the low-turbulence cases

considered. The spectrum, which is initialized with a von Karman-Pao profile, shows the position of the wave numbers corresponding to resolutions 9 and 17 grid points relative to the position of peak kinetic energy. The linear range (in the log plot) corresponds to the inertial range portion of the spectrum. Cases A and B fall within and at the limits of this inertial range, respectively.

The ODT resolution in a given direction is identical to that of DNS, which is 129 grid points. The layout of ODT elements is such they are aligned with the $17^3$ grid (case B). Therefore, the same distribution is adopted for both cases A and B, even though a layout of ODT elements in case A on the LES grid is found to be sufficient for the prediction of statistics of reactive scalars. In Case A, the ODT elements are placed on the LES grids as well as in between the LES grids. The number of ODT elements is specified in order to obtain sufficient statistics. In the present study, the choice of the number of ODT elements is also dictated by our interest in isolating the effects of the LES grid size.

## 4. Computational Cost

With the current ODT elements layout, the number of ODT grid points may be expressed as: $3 \times 129 \times 17^2$ or 111,843 grid points. Therefore, it only scales linearly with the DNS resolution in one direction; while, in DNS it scales with the cubic power of the DNS resolution in one direction. The factor of 3 represents the fact that three different directions for ODT domains are adopted within the lattice configuration. In contrast, the coarse-grid LES resolution is 729 and 4,913 grid points for cases A and B, respectively. Therefore, the bulk of the computational cost is in the ODT elements' solutions. Nonetheless, the total saving in total computational cells is, therefore, of the order of a factor of 20 times than that of DNS. This is a significant saving given that a lower number of gradients for advective and diffusive transport are also evaluated with ODT.

## V. RESULTS

Comparisons between LES-ODT and DNS results are based on both volume-averaged statistics and conditional statistics of thermo-chemical scalars. Volume-averaged statistics correspond to volume-averaged moments at a given instant in time of the simulation. These averages provide measures for the global evolution of the mixture, the progress of reaction and the evolution of key reactive scalars in the mixture. Conditional statistics are based on moments (primarily means and RMS values) at a given time of the simulation conditioned on the value of the mixture fraction. Conditional statistics provide further insight into finite-rate chemistry effects. For an acceptable outcome of the simulations, both sets of statistics must be consistent qualitatively and to a large extent quantitatively to statistics obtained from DNS.

## A. General Observations

Fig. 6 shows the evolution of isosurfaces of filtered values of the reaction progress variable, $c$, at 0.5 based on the high turbulence conditions at unity Lewis number. The evolution of the filtered progress variable marks the growth of autoignition kernels. Initially (not shown), no autoignition kernels are present. At $t$=0.2, the earliest autoignition kernels form, while more kernels form at a later time. The difference between early and late kernels is attributed primarily to the local rate of dissipation and the mixture conditions, which correspond to lean mixture conditions. The size of the nascent kernels is well below

the LES grid, and an elaborate statistical model is needed to predict conditions of autoignition at this stage. During intermediate stages of the autoignition process ($t$ = 0.8 and later), the expanding kernels begin to interact, and the initially closed kernels now form mangled autoignition fronts, which continue to burn through richer mixtures.

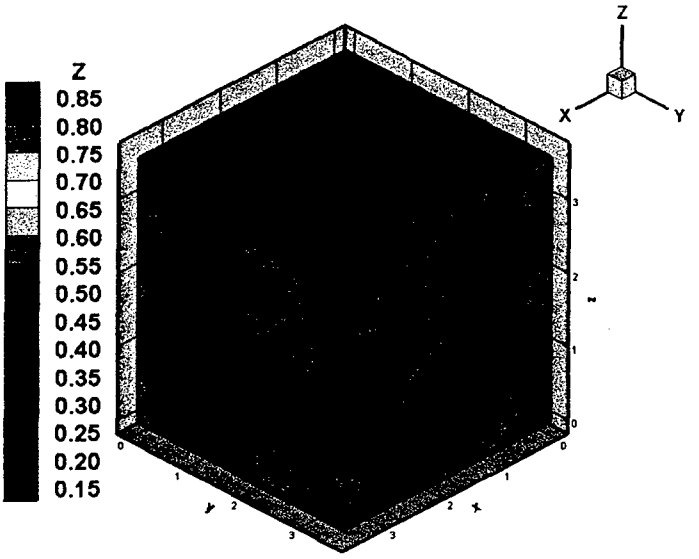


**Figure 4.** Initial mixture fraction field of the DNS solution. The same field is used to 'interpolate' the initial ODT solutions at $t$ = 0.

## B. Volume-Averaged Statistics

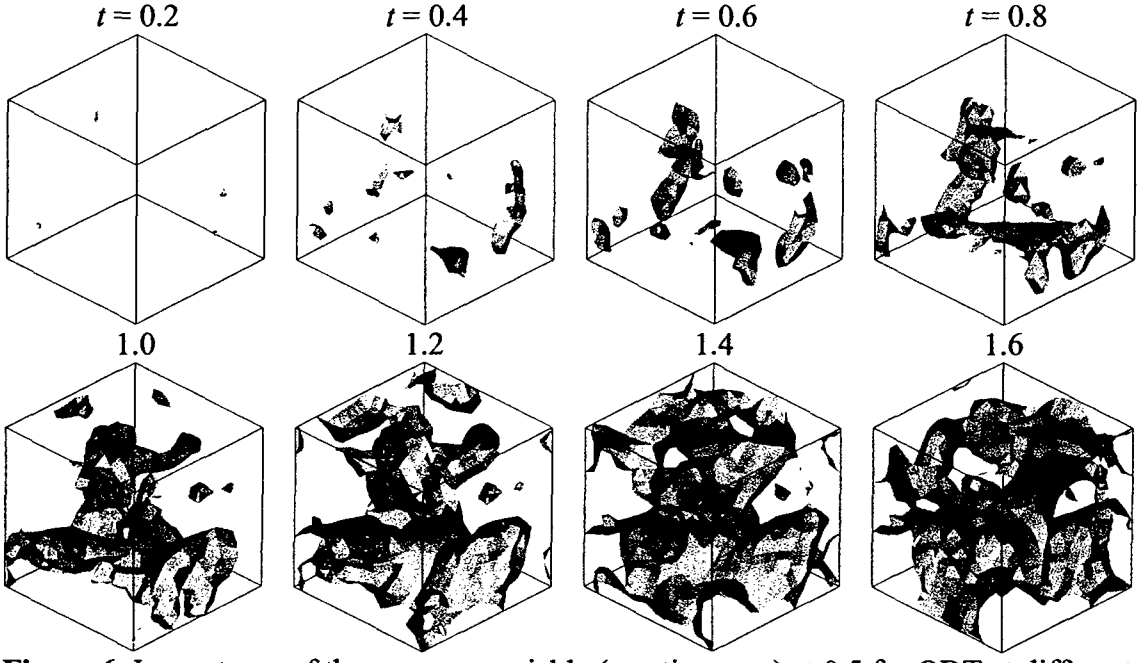


**Figure 6.** Isocontours of the progress variable (reacting case) at 0.5 for ODT at different times.

Fig. 7 shows the temporal evolution of the volume-averaged mean and RMS values of temperature, fuel mass fraction, and oxidizer mass fraction, respectively, between LES-ODT and DNS for the unity Lewis number case at both low and high turbulence conditions. The figure shows that both qualitative and quantitative trends of the mean values of these reactive species are well predicted by the LES-ODT approach; although an overall delay in the rates of completion of combustion can be observed for the high-turbulence case in the LES-ODT statistics. We have found, although we have not shown here, that this delay may be attributed entirely to events in LES-ODT of high dissipation that contributed to a delay in the auto-ignition process.

The most obvious differences between LES-ODT and DNS statistics are found in the RMS profiles at high-turbulence conditions. The inherent mechanism for these differences is related to the presence of ignition delay in high-dissipation kernels. Peaks in RMS, which are delayed for the high-turbulence LES-ODT statistics, reflect primarily the chemical activity and approximately coincide with peaks of mean reaction (not shown). Fuel mass fraction and temperature RMS are very similar. Because the evolution of the mixture fraction during the bulk of the combustion process occurs primarily in fuel lean conditions, the fuel represents the deficient species in the mixture, and rates of chemistry and associated changes in temperature also reflect fluctuations in this deficient species. The oxidizer RMS profiles are fundamentally different as shown at the bottom of Fig. 7, and are characterized by an initial rapid decay, then a second intermediate peak. In many respects, higher order statistics, such as the RMS, are expected to place the more stringent requirements on a model.

### C. Conditional Statistics

Figs. 7a-7d show conditional mean profiles of temperature vs. the mixture fraction at different stages of evolution of the autoignition process for the low-turbulence Lewis number case (Fig. 7a), and the high-turbulence cases of Lewis number of 0.5 (Fig. 7b), 1.0 (Fig. 7c), and 2.0 (Fig. 7d). Also shown are comparisons of the two different LES grid resolutions corresponding to resolution in the inertial and outside the initial range of the original turbulence spectrum. All figures show a steady decay in the range of the mixture fraction represented in the profiles as a function of time. This decay is observed in both LES-ODT and DNS-based statistics, and it may be attributed to the process of mixing, which eventually homogenizes the mixture. At later times of the mixture evolution, statistics eventually represent a narrow range around the stoichiometric mixture fraction, 0.5, which also corresponds to the condition of a homogeneous mixture at the end of the mixing process.

The profiles also show the evolution from a pure mixing linear profile with a negative slope indicating the initial preheating condition on the oxidizer side of the mixture. Increases beyond the initial peak value at $Z$ equal to 0 represent the onset of autoignition. These local peaks appear first at low mixture fractions indicating the onset of autoignition at fuel-lean mixtures. These peaks progressively move in both mixture fraction and physical spaces to richer conditions by lean premixed flame propagation. How far this peak will go into richer mixtures depends on the competing process of mixing.

The autoignition process is completed earlier for the high-turbulence case. Otherwise, a comparison between the evolution of the conditional mean profiles for temperature

between the low-turbulence and the high-turbulence cases indicates similar trends, albeit at a faster rate for the high-turbulence simulation. These trends are reproduced very well by the LES-ODT results. Perhaps an even more interesting comparison can be carried out between the various Lewis number cases in the high-turbulence computations. Figs. 7b-7c show that the case of Lewis number equal to 0.5 exhibits higher intermediate temperatures, followed by the unity Lewis number and the case of Lewis number equal to 2. These clear qualitative trends are reproduced equally in both the LES-ODT and DNS results. These trends are attributed to the fact that a lower Lewis number indicates a slower diffusion of "heat" relative to species. Therefore, an autoignition kernel is more shielded thermally from dissipation than species. In more practical mixtures and considering important differential (different diffusion rates between species) and preferential (different diffusion rates between species and enthalpy) diffusion effects, a non-unity Lewis number can result in either the loss of radicals or heat from these autoignition kernels. Considering the strong non-linear Arrhenius dependence on temperature compared to reactants, shielding of nascent kernels against heat loss would tend to increase the peak temperature in these kernels.

Figs. 8a-8d show conditional RMS profiles of temperature vs. the mixture fraction at different stages of evolution of the autoignition process for the low-turbulence Lewis number case (Fig. 8a), and the high-turbulence cases of Lewis number of 0.5 (Fig. 8b), 1.0 (Fig. 8c), and 2 (Fig. 8d). Also shown are comparisons of the two LES grid resolutions corresponding to resolution in the inertial and outside the initial range of the original turbulence spectrum. The range of the mixture fraction representing conditional statistics shrinks in time, reflecting the mixing process towards a homogeneous mixture. The figure shows very good predictions of the LES-ODT approach of temperature RMS at different times of the autoignition process and subsequent kernel growth. The predictions for higher turbulence conditions are very reasonable. The location of the peak temperature RMS is well predicted; but, some differences in magnitude of these peaks can be observed at early (at $t = 0.4$) and later stages ($t > 1.6$) of the autoignition process, while very good predictions are obtained otherwise. RMS profiles reflect primarily chemical activity. The figures show the propagation of ignition in phase and physical spaces from lean towards richer conditions. For the low turbulence case, peaks in temperature RMS are seen on the rich side of the mixture, as shown at times 2.4 and 3.6 in Fig. 8a. Because of the higher rates of mixing in the high-turbulence conditions, these peaks do not go beyond the stoichiometric condition of mixture fraction 0.5. As these peaks reach this stoichiometric condition, they eventually decay to zero when the combustion process is completed.

The higher temperatures associated with lower Lewis numbers at the high-turbulence conditions also are reflected in higher RMS values for the temperature at early stages of the autoignition process. This trend, however, is reversed at later times, as shown in profiles at $t = 2.4$ and 2.8. The same trends are exhibited by the LES-ODT and DNS statistics. These trends reflect the subtle coupling between the diffusion of "heat" and mass at non-unity Lewis numbers. While at early stages a Lewis number below unity helps to shield nascent autoignition kernels against thermal dissipation, the same process limits the transfer (or the preheat) of richer mixtures as the "propagation" of autoignition kernels evolve to these mixtures. Accordingly, reaction rates at rich mixtures are lower for lower Lewis numbers. This trend is illustrated clearly in the evolution of the conditional mean profiles of the reaction rate, $\omega$, for the same conditions features in Figs. 7 and 8, as shown in Figs. 9a-9d.

The profiles exhibit similar trends to those of the RMS profiles of temperature. Peak values of these conditional means are higher for the higher turbulence conditions at the same Lewis number of unity. The profiles show that these peaks evolve from lean conditions towards richer conditions. Perhaps the most subtle distinction between the low-turbulence and the high-turbulence conditions can be found at the later stages of the autoignition process ($t$ = 6.0 for low turbulence, and $t$ = 2.8 for high-turbulence). A single peak of the reaction rate remains for the low-turbulence conditions after the main mode of burning has swept through fuel-rich conditions. This peak reflects burning in the diffusion flame mode in contrast to the dominant peaks of burning on the lean and rich sides of the mixture. This peak has a significantly lower magnitude than the premixed flame burning mode, which is expected because of the fundamental burning mode differences between diffusion-based and premixed burning. This peak is not present in profiles of high-turbulence conditions. The representation of both premixed and non-premixed modes in both LES-ODT and DNS is an important indicator of the LES-ODT model fidelity in reproducing the salient physics of autoignition in non-homogeneous mixtures.

A comparison among the profiles at high turbulence conditions for the various Lewis numbers shows that the lower Lewis number condition exhibits higher peaks initially, and then lower peaks as the combustion process propagates towards richer mixtures. At these conditions, the higher Lewis number case exhibits higher mean reaction rates as shown at the later times of 2.0, 2.4 and 2.8. The difference among the Lewis number cases reflects the strong sensitivity of the reaction rate to temperature and the role of the Lewis number in thermal dissipation in the nascent autoignition kernels.

## V. Conclusions

A new framework for large-eddy simulation of turbulent combustion was proposed. The framework is based on coupling LES solvers with low-dimensional stochastic models in general and have been presented for the One-Dimensional Turbulence (ODT) model. The principal advantage of the ODT formulation is that terms in the governing equations of LES for the transport of momentum, energy and scalars can be represented in 1D through a hybrid scheme of deterministic and stochastic contributions. Another important advantage of the ODT formulation is that processes of molecular transport, chemistry and turbulent transport are closely coupled to address a broad class of problems in turbulent combustion. The resulting governing equations of ODT are designed to be consistent with their filtered counterparts Additional advantages of the proposed framework have been outlined in the body of the report.

A second important implementation involve the formulation of a LES-ODT model within the proposed framework designed to solve for scalars, while the momentum equations are handled with a "standard" LES model; therefore, the formulation targets closure for physics that has been the scope of turbulent combustion models for more than 30 years, including the modeling of non-linear reaction source terms and the prediction of reactive scalar statistics. The formulation was implemented in a canonical problem that features physics relevant to some of the outstanding questions in turbulent combustion models. The problem is based on non-homogeneous autoignition, where ignition occurs at discrete ignition sites well below the LES grid resolution. Conditions of ignition are based on local conditions of dissipation and mixture, which too are not resolved on the LES grid. A consistent agreement with DNS at varying turbulence conditions and in the presence of preferential

diffusion effects is found. The validation provided a demonstration of the capability of the LES-ODT model and the proposed framework in general. Future extensions to the model are needed to establish it as a viable tool for predicting the behavior of turbulent reacting flows in practice.

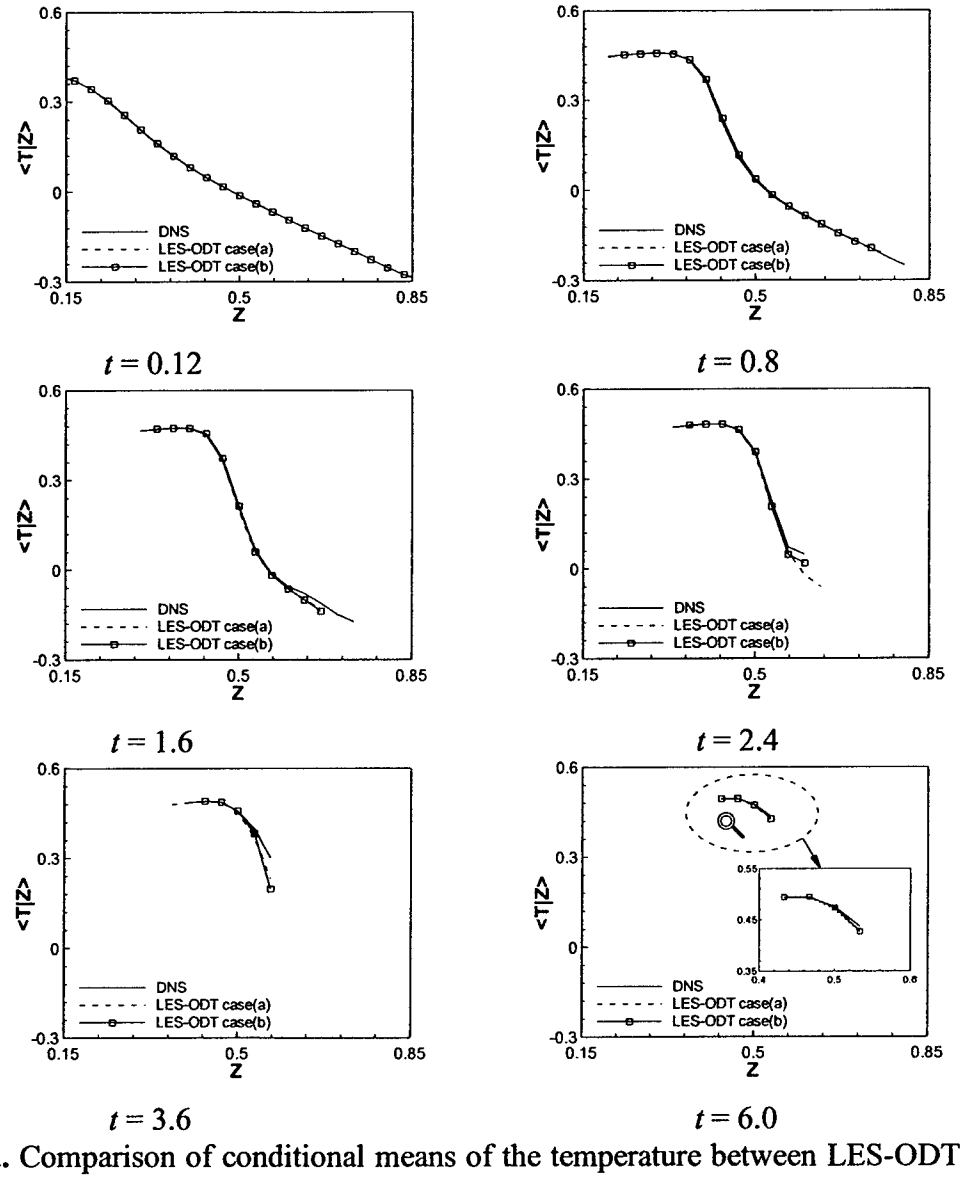


**Figure 7a.** Comparison of conditional means of the temperature between LES-ODT and DNS at different times for the low turbulence case with $Le = 1$.

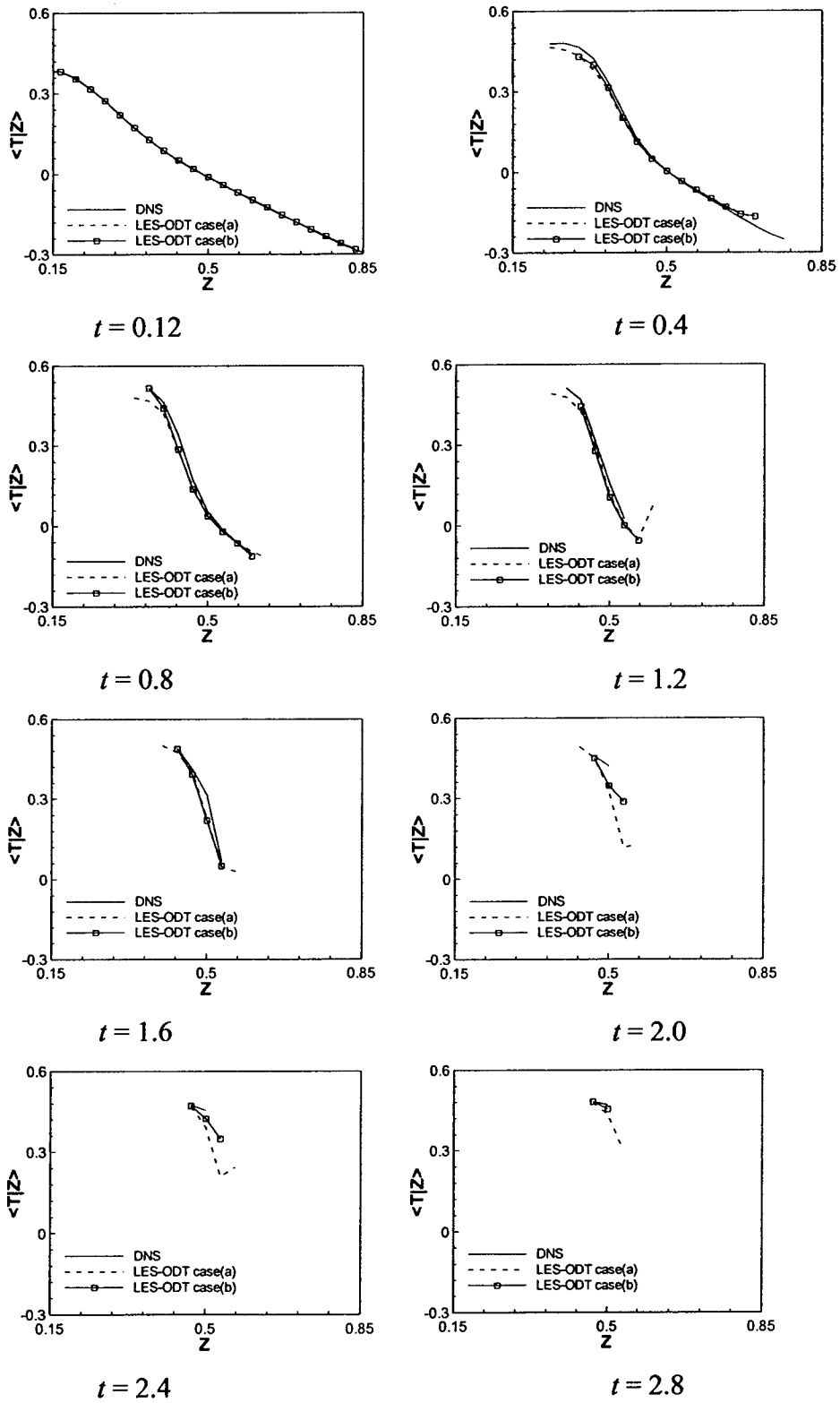


**Figure 7b.** Comparison of conditional means of the temperature between LES-ODT and DNS at different times for the high turbulence case with $Le = 0.5$.

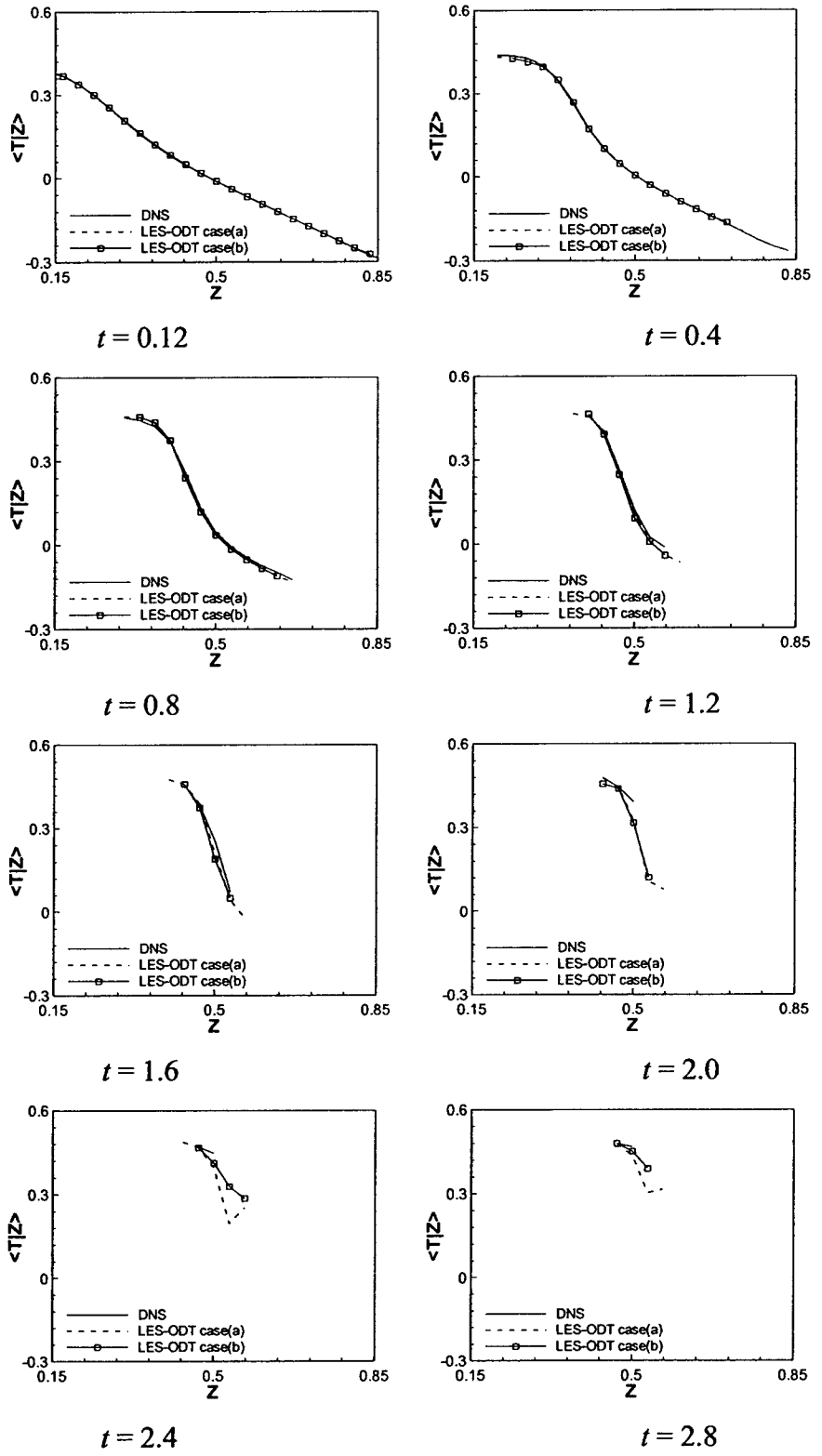


**Figure 7c.** Comparison of conditional means of the temperature between LES-ODT and DNS at different times for the high turbulence case with $Le = 1.0$.

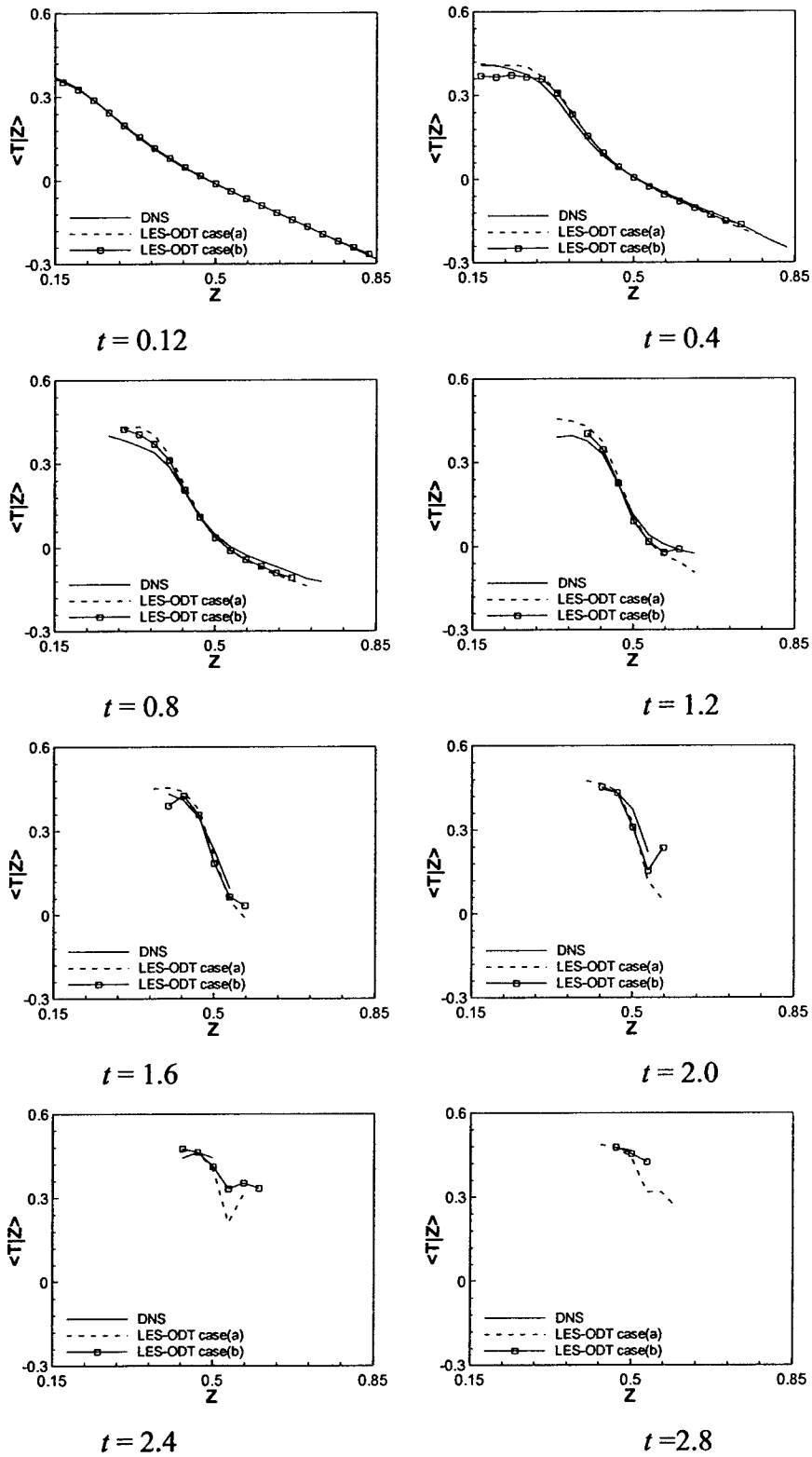


**Figure 7d.** Comparison of conditional means of the temperature between LES-ODT and DNS at different times for the high turbulence case with $Le = 2.0$.

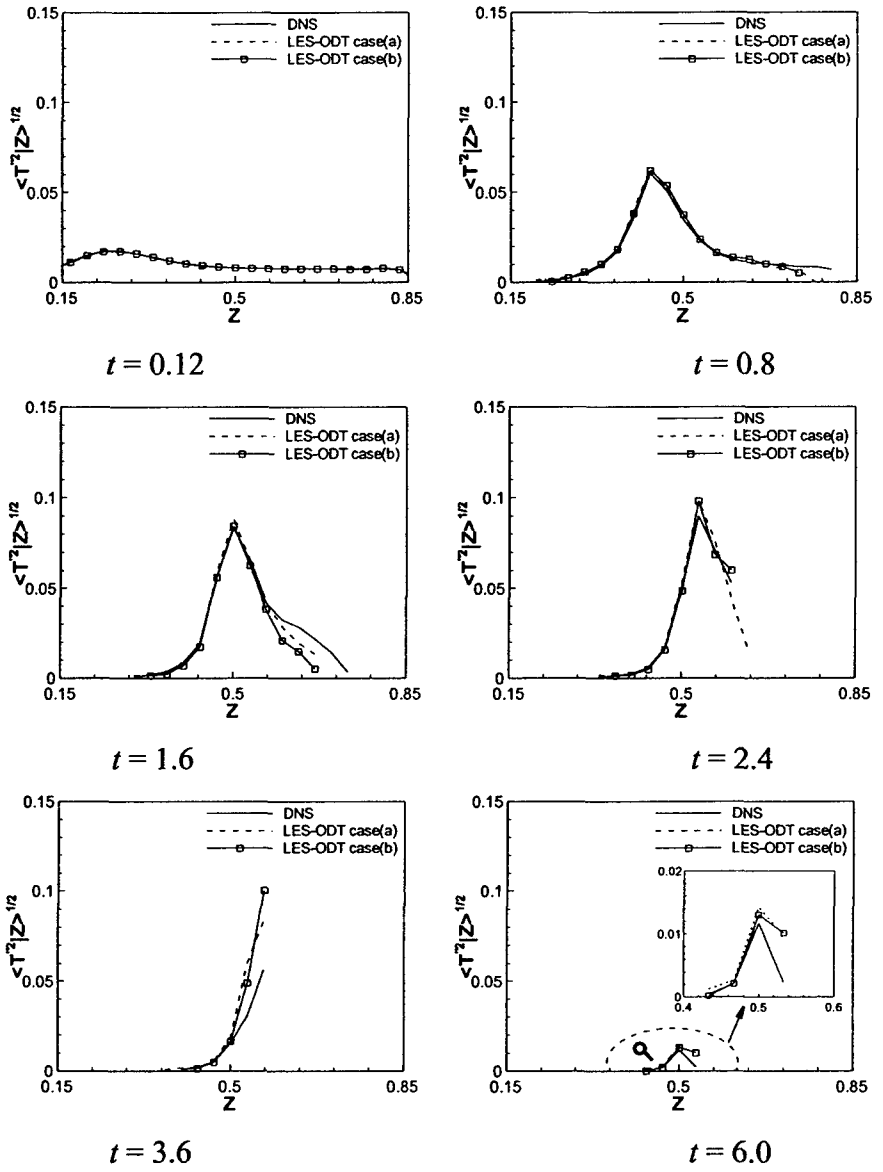


**Figure 8a.** Comparison of conditional RMS of the temperature between LES-ODT and DNS at different times for the low turbulence case with $Le = 1$.

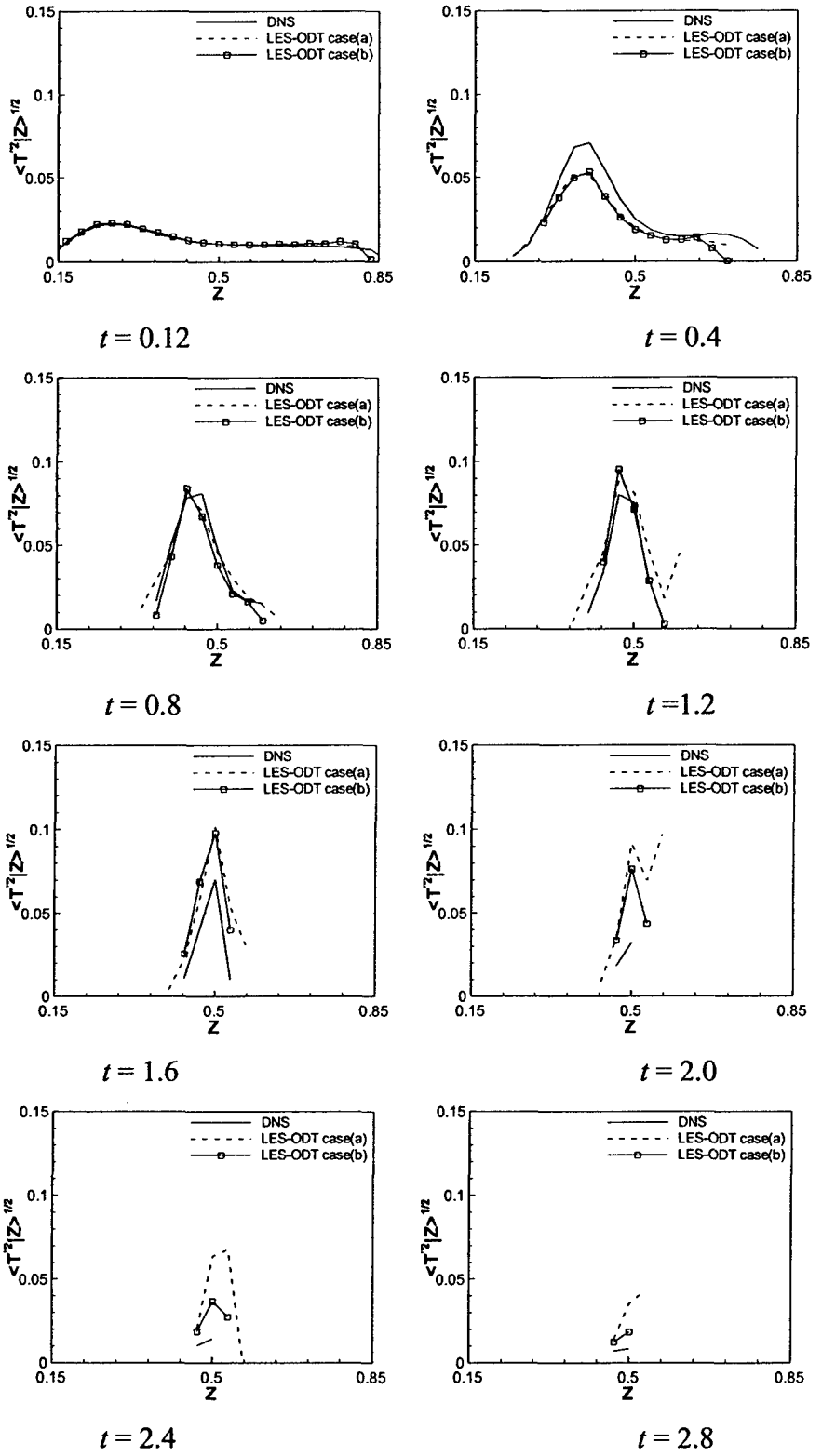


**Figure 8b.** Comparison of conditional RMS of the temperature between LES-ODT and DNS at different times for the high turbulence case with $Le = 0.5$.

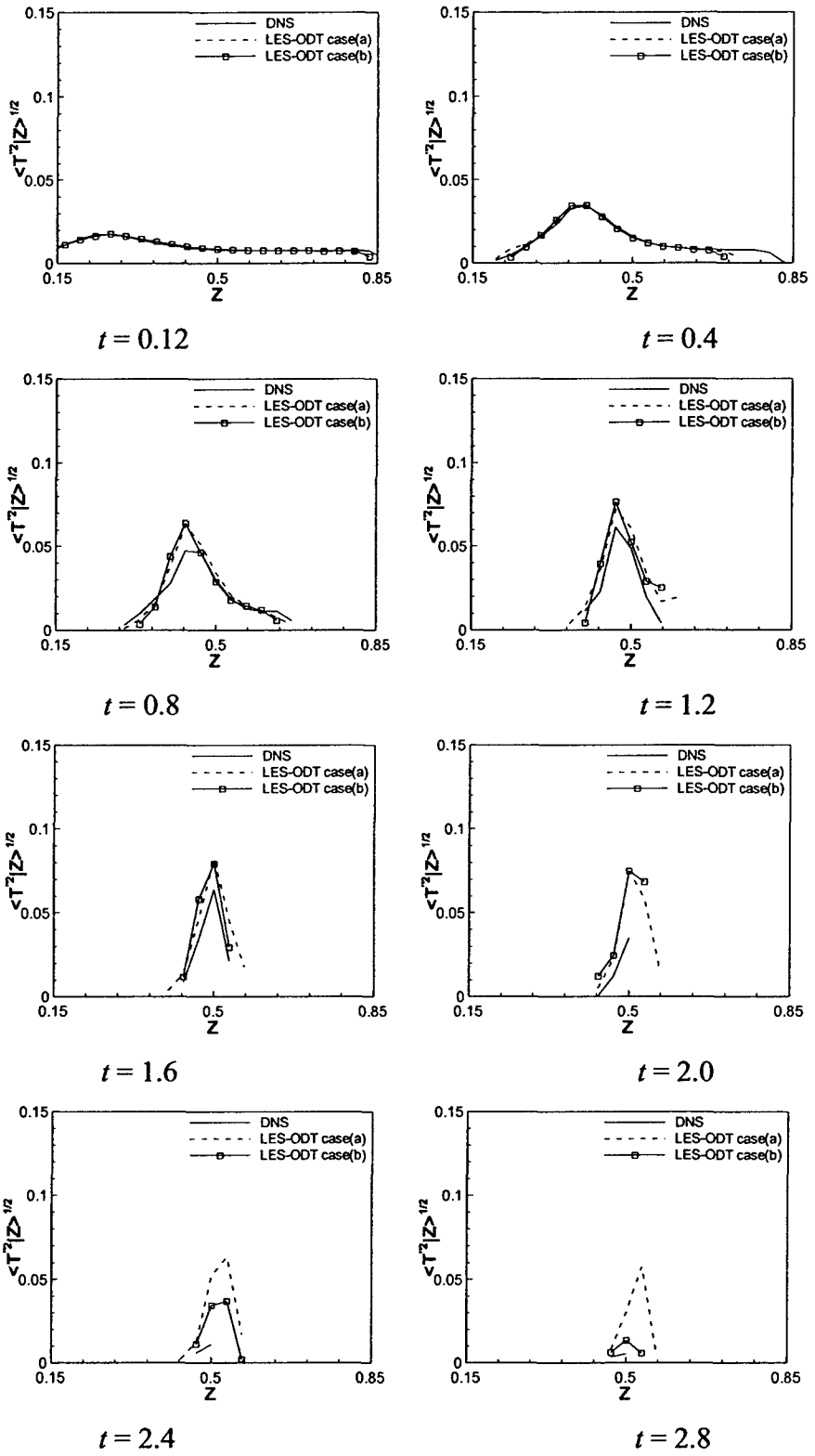


**Figure 8c.** Comparison of conditional RMS of the temperature between LES-ODT and DNS at different times for the high turbulence case with $Le = 1.0$.

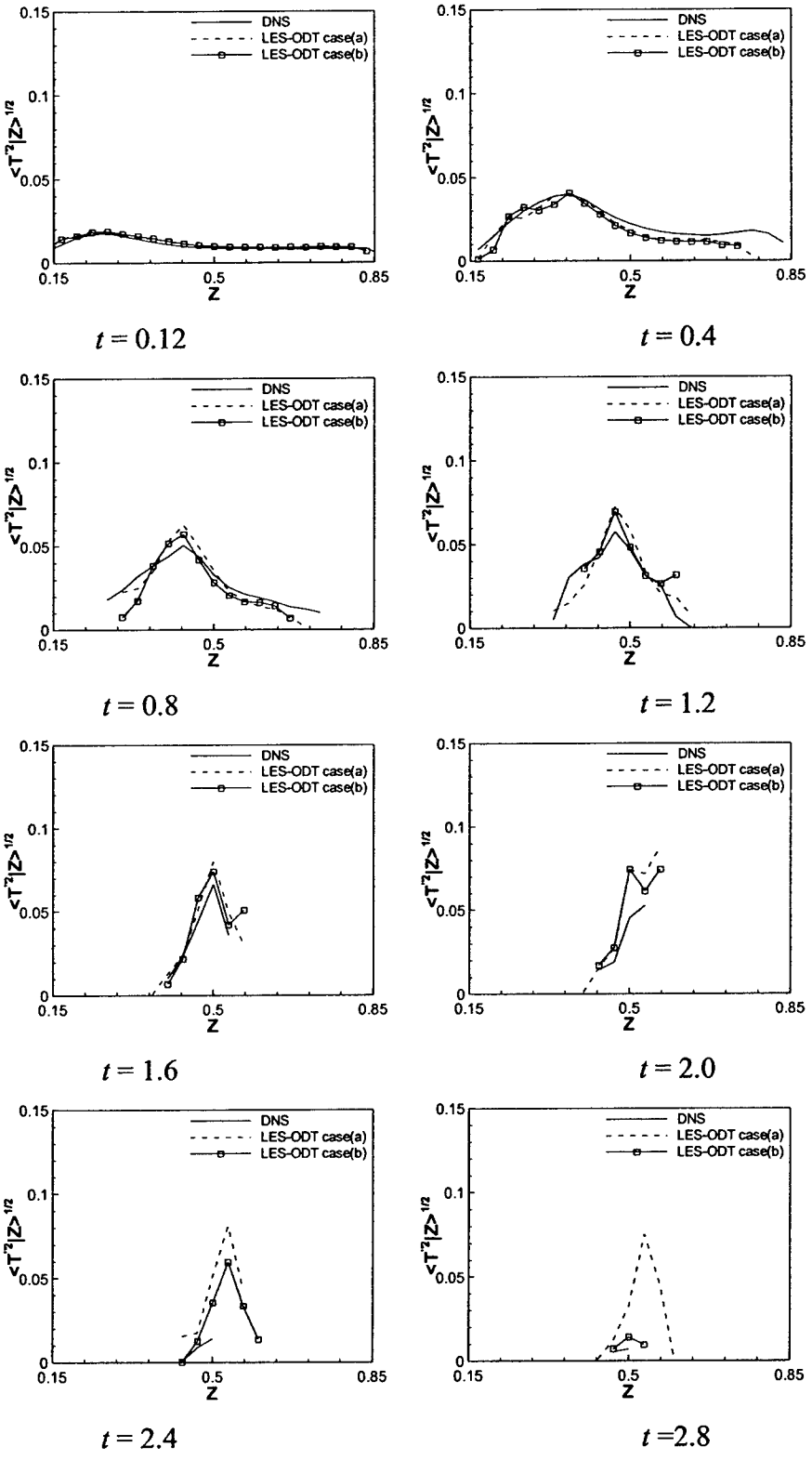


**Figure 8d.** Comparison of conditional RMS of the temperature between LES-ODT and DNS at different times for the high turbulence case with $Le = 2.0$.

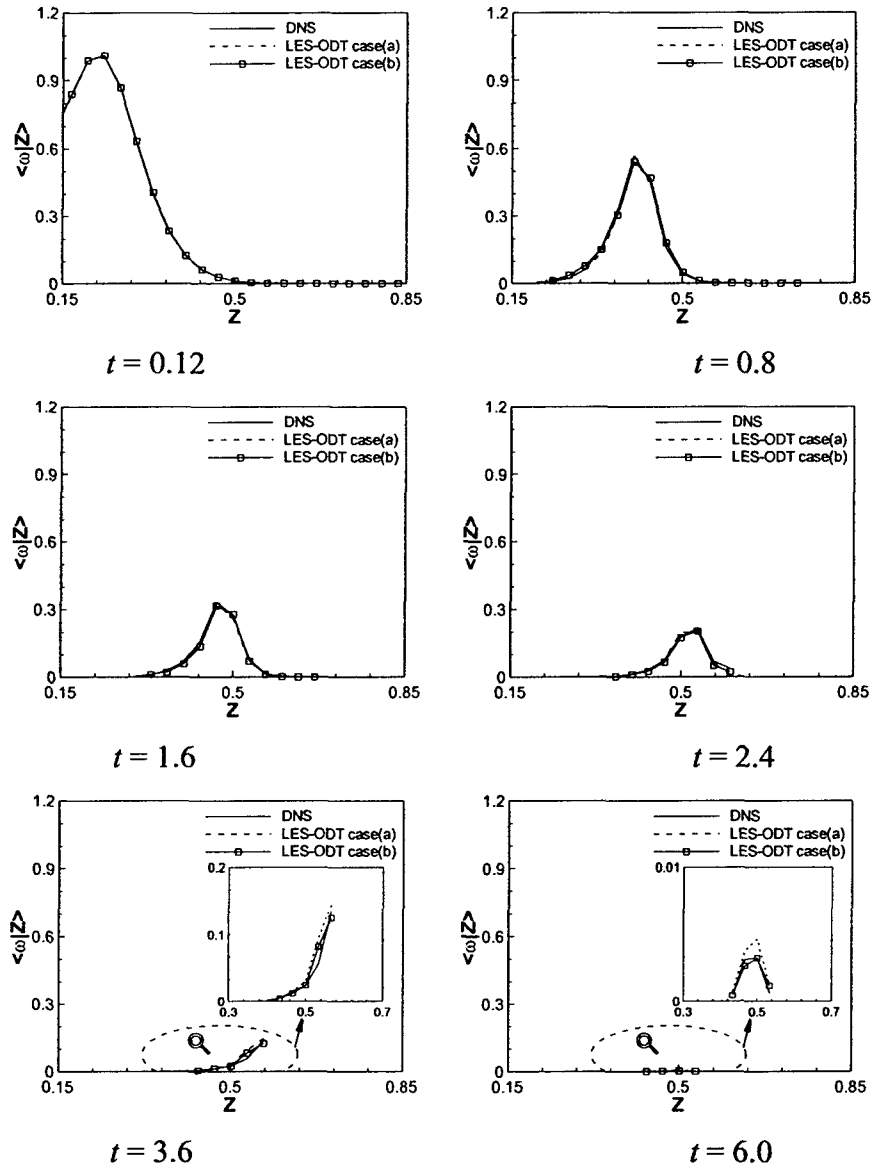


**Figure 9a.** Comparison of conditional means of the reaction rate between LES-ODT and DNS at different times for the low turbulence case with $Le = 1$.

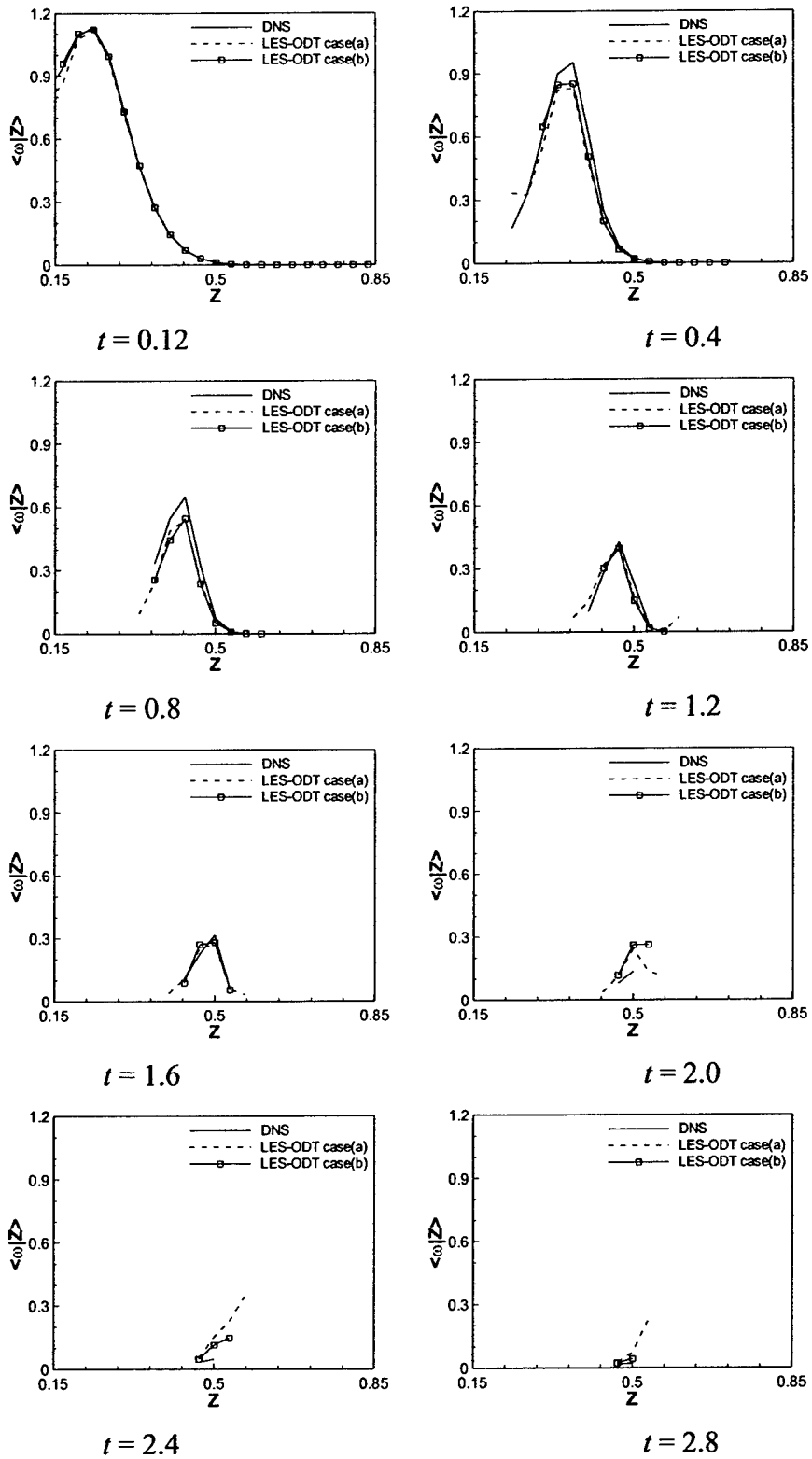


**Figure 9b.** Comparison of conditional means of the reaction rate between LES-ODT and DNS at different times for the high turbulence case with $Le = 0.5$.

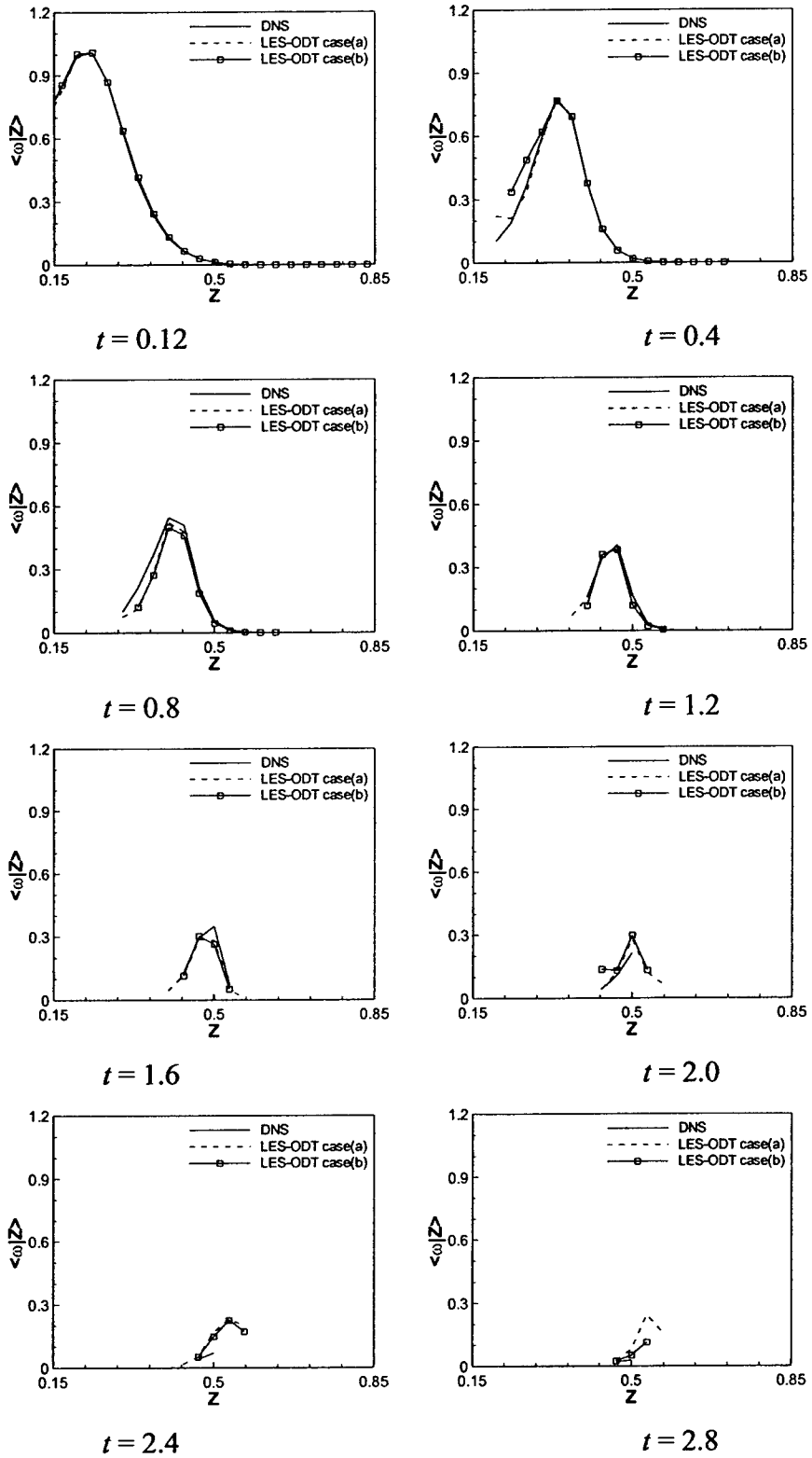


**Figure 9c.** Comparison of conditional means of the reaction rate between LES-ODT and DNS at different times for the high turbulence case with $Le = 1.0$.

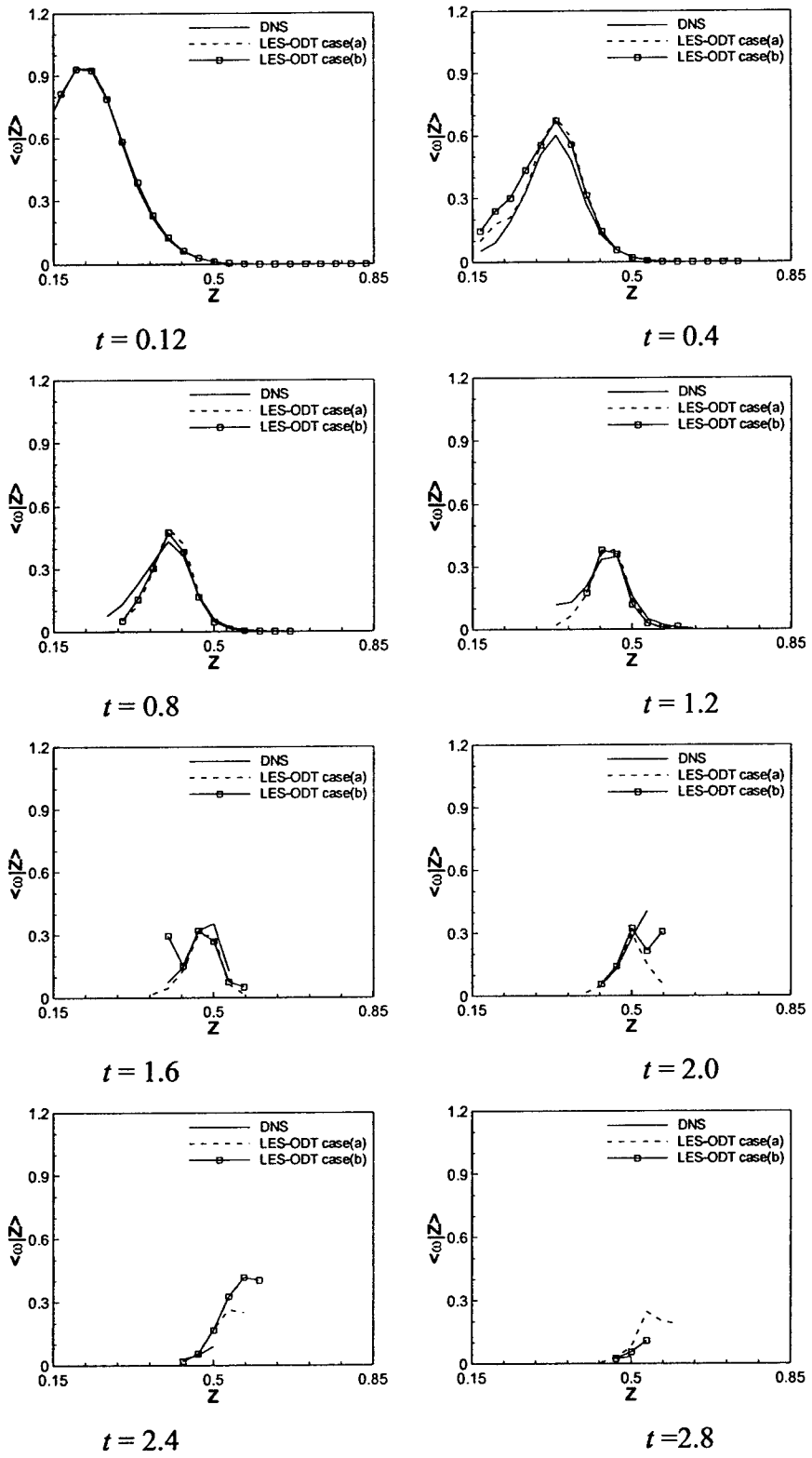


**Figure 9d.** Comparison of conditional means of the reaction rate between LES-ODT and DNS at different times for the high turbulence case with $Le = 2.0$.

## References


Caldeira-Pires, A., and Heitor, M.V., Characteristics of turbulent heat transport in nonpremixed jet flames, *Combust. Flame* **124**, 213-224 (2001).

Calhoon, W.H., and Menon, S., Subgrid modeling for reacting large eddy simulations, *AIAA 96-0516* (1996).

Calhoon, W.H., and Menon, S., Linear-eddy subgrid model for reacting large-eddy simulations: heat release effects, *AIAA 97-0368* (1997).

Chakravarthy, V.K., and Menon, S., Subgrid modeling of turbulent premixed flames in the flamelet regime, *Flow, Turbul. Combust.* **65**, 133-161 (2000).

Chakravarthy, V.K., and Menon, S., Linear eddy simulations of Reynolds number and Schmidt number effects on turbulent scalar mixing, *Phys. Fluids* **13**, 488-499 (2001).

Colucci, P.J., Jaberi, F.A., Givi, P., and Pope, S.B., Filtered density function for large eddy simulation of turbulent reacting flows, *Phys. of Fluids* **10**, 499-515 (1998).

Dreeben, T.D., and Kerstein, A.R., Simulation of vertical slot convection using 'one-dimensional turbulence', *Int. J. Heat Mass Tran.* **43**, 3823-3834 (2000).

Echekki, T., Kerstein, A.R., Dreeben, T.D., and Chen, J.Y., 'One-Dimensional Turbulence' Simulations of Turbulent Jet Diffusion Flames: Model Formulation and Illustrative Applications, *Combust. Flame* **125**, 1083-1105 (2001).

Germano, M., Turbulence: the filtering approach, *J. Fluid Mech.* **238**, 325-336 (1992).

Geurts, B.J., Inverse modeling for large-eddy simulation, Phys. Fluids 9, 3585-3587 (1997).

Giquel, L.Y.M., and Givi, P., Velocity filtered density function for large eddy simulation of turbulent flows, *Phys. Fluids* **14**, 1196-1213 (2002).

Hewson, J.C., and Kerstein, A.R., Stochastic simulation of transport and chemical kinetics in turbulent CO/H2/N2 flames, *Combust. Theo. Model.* **5**, 669-697 (2001).

Hewson, J.C., and Kerstein, A.R., Local extinction and reignition in nonpremixed turbulent CO/H2/N2 jet flames, *Combust. Theo. Model.* **5**, 669-697 (2001).

Hewson, J.C., Kerstein, A.R., and Echekki, T., One-dimensional stochastic simulation of advection-diffusion-reaction couplings in turbulent combustion, in Turbulent Mixing and Combustion (Pollard, A. and Candel, S., Eds.), Kluwer Academic Publishers, The Netherlands, 2002.

Jaberi, F.A., Collucci, P.J., James, S., and Givi, P., Filtered mass density function for large eddy simulation of turbulent reacting flows, *J. Fluid Mech.* **401**, 85 (1999).

Jaberi, F.A, Miller, R.S., Madnia, C.K., Givi, P., Non-Gaussian scalar statistics in homogeneous turbulence, *J. Fluid Mech.* **313**, 241-282 (1996).

Kerstein, A.R., Linear-Eddy Modeling of Turbulent Transport 2. Applications to Shear-Layer Mixing, *Combust. Flame* **75**, 397-413 (1989).

Kerstein, A.R., Linear-Eddy Modeling of Turbulent Transport 3. Mixing and Differential Molecular-Diffusion in Round Jets, *J. Fluid Mech.* **216**, 411-435 (1990).

Kerstein, A.R., Linear-Eddy Modeling of Turbulent Transport 6. Microstructure of Diffusive Scalar Mixing Fields, *J. Fluid Mech.* **231**, 361-394 (1991).

Kerstein, A.R., Linear-Eddy Modeling of Turbulent Transport 4. Structure of Diffusion Flames, *Combust. Sci. Tech.* **81**, 75-96 (1992).

Kerstein, A.R, McMurtry, P.A., Low-Wave-Number Statistics of Randomly Advected Passive Scalars, *Phys. Review E* **50** , 2057-2063, 1994.

Kerstein, A.R., One-dimensional turbulence: model formulation and application to homogeneous turbulence, sheer flows, and buoyant stratified flows, *J. Fluid Mech.* **392**, 277-334 (1999a).

Kerstein, A.R., One-dimensional turbulence Part 2. Staircases in double-diffusive convection, *Dyn. Atmos. Oceans* **30**, 25-46 (1999b).

Kerstein A.R., Ashurst, W.T., Wunsch, S., Nilsen, V. , One-dimensional turbulence: vector formulation and application to free shear flows, *J. Fluid Mech.* **447**, 85-109 (2001).

Kerstein, A.R., and Dreeben, T.D., Prediction of turbulent free shear flow statistics using a simple stochastic model, *Phys. Fluids* **12**, 418-424 (2000).

Kerstein, A.R., One-Dimensional Turbulence: A new approach to high-fidelity subgrid closure of turbulent flow simulations, *Comput. Phys. Commun.*, Vol. 148(1), 1-16 (2002).

Mason, S.D., Turbulent transport in spatially developing reacting shear layers, Ph.D. Thesis, Department of Mechanical Engineering, University of Wisconsin, 2000.

Mason, S.D., Rutland, C.J., Turbulent transport in spatially developing reacting shear layers, *Proc. Combust. Inst.* **28**, 505-513 (2000).

McDermott, R.J., Kerstein, A.R., Schmidt, R.C., and Smith, P.J., The ensemble mean limit of the one-dimensional turbulence model and application to residual stress closure in finite volume large-eddy simulation, J. Turbul., 6, No. 31, 1-33, 2005.

McMurtry, P.A., Menon, S., and Kerstein, A.R., A linear eddy sub-grid model for turbulent reacting flows: applications to hydrogen-air combustion, *Proc. Combust. Inst.* **24**, 271-278 (1992).

Menon, S., McMurtry, P.A., and Kerstein, A.R., A linear eddy mixing model for large eddy simulation of turbulent combustion in *Large Eddy Simulation of Complex Engineering and Geophysical Flows*, (B. Galperi and S.A. Orszag, Eds.), Cambridge University Press, New York, 1993, 287-314.

Oran, E.S., and Boris, J.P., Numerical simulation of reactive flow, Second Edition, Cambridge University Press (2001).

Peters, N., *Turbulent Combustion*, Cambridge University Press, Cambridge, UK, 2000.

Peters, N., Laminar Flamelet Concepts in Turbulent Combustion, *Proc. of the Combust. Inst.* **21**, 591-612 (1988).

Pitsch, H., Large-Eddy Simulation of Turbulent Combustion, Ann. Rev. Fluid mech., 38, 453-482, 2006.

Pope, S.B., PDF Methods for Turbulent Reacting Flows, *Prog. Energy Combust. Sci.* **11**, 119-192 (1985).

Pope, S.B., Computations of turbulent combustion: progress and challenges, *Proc. Combust. Inst.* **23**, 591-612 (1990).

Pope, S.B., Turbulent Flows, Cambridge University Press, Cambridge, UK, 2000.

Sankaran, V., and Menon, S., Structure of premixed turbulent flames in the thin-reaction-zones regime, *Proc. Combust. Inst.* **28**, 203-209 (2000).

Schmidt, R.C., Kerstein, A.R., Wunsch, S., and Nilsen, V.J., Near-wall LES closure based on one-dimensional turbulence modeling, *J. Comput. Phys.* **186**, 317-355 (2003).

Sheikhi, M.R.H., Drozda, T.G., Givi, P., Pope, S.B., Velocity-scalar filtered density function for large eddy simulation of turbulent flows, *Phys. Fluids* **15**, 2321-2337 (2003)

Smagorinsky, J.S., General circulation experiments with the primitive equations, I, the basic experiment, *Mon. Weather Rev.* **91**, 99-164 (1963).

Smith, T.M., and Menon, S., Large-eddy simulations of turbulent reacting stagnation point flows, AIAA 97-0372 (1997).

Smith, T.M., and Menon, S., Subgrid combustion modeling of premixed turbulent reacting flows, AIAA-98-0242 (1998).

Veynante, D., Trouvé, A., Bray, K.N.C., and Mantel, T., Gradient and countergradient diffusion in turbulent premixed flames, *J. Fluid Mech.* **332**, 263-293 (1997).

Wunsch, S., and Kerstein, A.R., A model for layer formation in stably stratified turbulence, *Phys. Fluids* **13**, 702-712 (2001).

## Personnel Supported

The following personnel have been supported through the grant:
Prof. Tarek Echekki, PI
Shufen Cao, Ph.D. student
Bhargav Ranganath, Ph.D. student
Sha Zhang, M.S. student
Caixa Chen, Post-Doctoral Fellow

## Degrees Granted

Sha Zhang, M.S. August 2003
Shufen Cao, Ph.D August 2006.
Bhargav Ranganath, December 2006 (anticipated)

## Meeting Participation

March 16-19, 2003 - Third Joint Meeting of the U.S. Sections of the Combustion Institute, Chicago, IL.

June 23-25, 2003 – ARO-AFOSR Contractors Meeting in Chemical Propulsion, Williamsburg, VA.

May 9-12, 2004 – Tenth International Conference on Numerical Combustion, Sedona, AZ.

June 7-9, 2004 – ARO-AFOSR Contractors Meeting in Chemical Propulsion, Tuscon, AZ.

March 20-23, 2005 – Fourth Joint Meeting of the U.S. Section of the Combustion Institute, Drexel University, Philadelphia.

June 20-22, 2005 – ARO-AFOSR Contractors Meeting in Chemical Propulsion, Indianapolis, IN.

## Interaction with AFRL

Discussions with Dr. Campbell Carter at AFRL were held during the ARO-AFOSR contractors meetings as well through e-mail communications. We explored strategies for the establishment of experimental measurements that explore spatial filtering of PLIF data within the context of LES and the potential use of computational validation through DNS.

## Technology Transition and Transfers

N/A

## Honors and Awards

None

## Inventions and Patents

None

## List of Submitted and Accepted Publications during the Reporting Period

(a list and files of submitted publications sponsored by the grant will be posted using the following link:
http://www.mae.ncsu.edu/homepages/echekki/lesodtpub.htm)

Ranganath, B. and Echekki, T., One-Dimensional Turbulence-based closure for turbulent non-premixed flames, Progress in Computational Fluid Dynamics, Vol. 6, pp. 409-418 (2006).

Cao, S. and Echekki, T., Autoignition in non-homogeneous mixtures: conditional statistics and implications for modeling, Submitted to Combustion and Flame, 2006.

Cao, S. and Echekki, T., A structure-based approach for the large-eddy simulation of combustion based on the one-dimensional turbulence model, Submitted to Physics of Fluids, 2006.

### Conference Papers

Zhang, S. and Echekki, T., One-Dimensional Turbulence simulation of turbulent jet diffusion flames of hydrogen wih helium dilution, Third Joint Meeting of the U.S. Sections of the Combustion Institute, Chicago, March 16-19, 2003.

Cao, S. and Echekki, T., 3D Simulation of Autoignition in Non-Homogeneous Mixtures in Homogeneous, Isotropic Turbulence and Validation with the Conditional Moment Closure Model, Presented at the Fourth Joint Meeting of the U.S. Sections of the Combustion Institute, Philadelphia, PA, 2005.